Experimental Validations of a Low-Boom Aircraft Design

Todd E. Magee[1]
Boeing Research and Technology, Huntington Beach, CA, 92647, USA

Stephen G. Shaw[2]
Boeing Commercial Airplanes, Seattle, WA, 98124, USA

and

Spencer R. Fugal[3]
Boeing Research and Technology, Seattle, WA, 98124, USA

A two-phase study is described that designs and validates a supersonic airliner feasible for entry into service in the 2018 to 2020 timeframe (NASA N+2 generation). A Mach 1.6 to 1.8 low sonic-boom aircraft configuration is developed that meets aggressive sonic-boom and performance goals. The concept and the tools utilized for its design are validated through a series of wind-tunnel tests at the NASA Ames 9 ft x 7 ft Supersonic Wind Tunnel, NASA Ames 11 ft Transonic Wind Tunnel, and NASA Glenn 8 ft x 6 ft Supersonic Wind Tunnel. Comparisons between CFD and wind-tunnel near-field pressure distributions are made. Sonic-boom test techniques are described and investigated. Results from spatial-averaging show the best agreement with CFD.

Nomenclature

2D	Two-Dimensional
3D	Three-Dimensional
765-076E	Boeing N+ 2 System Study baseline concept
AOA	Angle-of-Attack
BOR	Body-of-Revolution
CA	Axial Force Coefficient
CD	Drag Coefficient
CFD	Computational Fluid Dynamics
CL	Lift Coefficient
CM	Pitching Moment Coefficient
CN	Normal Force Coefficient
DP/P	(P-Pinf)/Pinf
DPOVP AVG_Y	Averaged (P-Pinf)/Pinf with the reference pressure run removed
DPOVPU AVG_Y	Averaged (P-Pinf)/Pinf with the reference pressure run not removed
H	Height

[1] Principal Investigator, Flight Sciences, 5301 Bolsa Ave/MC H017-D334, AIAA Senior Member
[2] Aerodynamics Engineer, Product Development, P.O. Box 3707/MC OR-MM
[3] Aerodynamics Engineer, Flight Sciences, P.O. Box 3707/MC OR-MM

H/L	Height/Length
L/D	Lift-to-Drag ratio
MDA	Multi-Disciplinary Analysis
MDBOOM	A Boeing linear wave propagation code based on the Thomas method
MDO	Multi-Disciplinary Optimization
MDOPT	A Multidisciplinary Design OPTimization system
NASA	National Aeronautics and Space Administration
OVERFLOW	The OVERset grid FLOW solver. This code solves the Reynolds-Averaged Navier-Stokes equations
PLdB	Perceived Loudness in decibels
QEVC	Quiet Experimental Validation Concept
SEEB	Seebass and George minimum sonic boom theory (equivalent area body of revolution)
SSBD	Shaped Sonic Boom Demonstrator
WT Re	Wind-Tunnel Reynolds Number
x/L	Axial location/Length
Zephyrus	Boeing sonic boom propagation computer code that predicts the expected sonic boom waveform at ground level using the extended Burger's equation

I. Introduction

After decades of research and development, it is now possible to design an aircraft shape that has both a low sonic-boom signature and reasonable performance. The groundwork, theory, and methods behind low sonic-boom aircraft design were initially developed by Seebass and George [1, 2, and 3] in 1969 and further developed by Darden [4, 5] in 1975. However, these methods did not generate realistic aircraft configurations because of the limitation of the linear methods and computing at that time. The configurations developed were generally point designs and were a compromise between the boom goals and the aerodynamic performance goals.

In the last 10 years significant improvements in low-boom design, CFD, and computer power have resulted in the ability to generate low-boom aircraft that meet both goals. CFD-based shape optimization has been a key ingredient in meeting both the sonic-boom and aerodynamic performance goals. Some of the leading CFD-based sonic-boom shape optimization tools include the Cart3D adjoint code by Aftosmis [6] and the FUN3D adjoint/sBOOM tool by Park/Rallabhandi [7, 8]. These tools couple parametric geometry, CFD near-field flow solutions, wave propagation, and ground-level sound metric computation into a single design tool with sonic-boom and performance as the objective function. The adjoint formulation results in the ability to compute sensitivities for hundreds of design variables during a single design optimization, which is required to effectively shape a low sonic-boom aircraft.

The key unknown is the validity of the low-boom signatures provided by these new low-boom design and analysis tools. Do the aircraft configurations designed by these tools have the predicted near-field and ground signature shape and magnitude? How accurate are the results? Ground and flight test validation is required to answer these questions. In 2003, the DARPA Quiet Supersonic Platform (QSP) Shaped Sonic Boom Demonstrator (SSBD) program [8] showed that a shaped near-field signature does persist to the ground. In this flight experiment the front portion of an F-5E fuselage was modified to produce a shaped front-side ground signature. The aft portion of the aircraft and its aft signature were not modified. Thus, the aft portion of the signature was still a classic N-wave. Although the SSBD had a shaped front signature, it was not considered low-boom. This was a key first step, but additional design and validation work is required to lift the ban on commercial supersonic flight overland. Since 1973, the FAA has banned civil supersonic flight (or the sonic boom from reaching the ground) over the continental United States (FAA Part 91.817) without a specific waiver. The only way to obtain a waiver and lift the ban is to develop aircraft that have acceptable shaped low-boom signatures. The shaped signatures for these aircraft must be

validated with both wind-tunnel testing and flight testing to ensure that they are truly achieving the sonic-boom goals before seeking public acceptance.

The objective of this paper is to detail the sonic-boom and aerodynamic performance validation work that has been conducted under the auspices of the NASA N+2 System-Level Experimental Validation project. This project includes the development of a low sonic-boom aircraft concept using CFD-based shape optimization tools and the validation of the concept and tools in a relevant wind-tunnel environment. The main areas that will be detailed in this report include a summary of the project goals and objectives, low-boom design methodology, wind-tunnel models and test program, validation analyses, and results including test techniques and their limitations, and remaining work.

II. N+2 Experimental Validation Program

The N+2 Experimental Validation program is a 3-year NASA funded program that is broken down into two 18-month phases. Each phase of the project is comprised of four major tasks. First, an aircraft configuration is designed to meet specific sonic-boom and performance goals. Next, the concept is analyzed using CFD. Then wind-tunnel models of the concept are fabricated and tested in the wind tunnel. Finally, the wind-tunnel data is compared with the analytical results. Phase I of the program is focused specifically on the sonic-boom and performance of the total aircraft configuration, whereas Phase II is focused on the effect of propulsion (inlet and nozzle) integration on the sonic-boom and performance. The work for Phase I is complete while Phase II is in progress.

The project goals are outlined in Table 1. The sonic-boom goal is the highest priority. The ground signature of the low-boom concept must have front and aft signature shaping and must have a perceived loudness level of 85 PLdB or less. The L/D and range goal are the second priority and must be as good or better than the 765-076E configuration that was developed under the NASA N+2 Systems Study. A description of this work is found in Welge et al. [9]. The remaining N+2 goals are listed in the figure, but are tradeable. The cruise Mach number was determined during Phase I of the contract based on boom shaping and model support concerns. A Mach number of 1.8 has been identified as the baseline, but a Mach 1.6 concept has also been carried along throughout the project. During the design process, all of the major disciplines (performance, aerodynamics, stability, mass properties, sonic-boom, and propulsion) have been assessed. However, only the sonic-boom and performance areas are required to meet the goals. If a particular discipline (other than sonic-boom or performance) does not meet goals/expectations, it is noted for future development work. The objective here is to generate an Outer-Mold-Line (OML) to validate low-boom shaping design methods and tools, and not to create a mature product concept.

Objective	Goal Value
Sonic-Boom (PLdB)	85 PLdB with front and aft signature shaping
Lift / Drag Ratio	As good as the Boeing 765-076E
Range (nmi)	4,000
Mach Number	1.6 – 1.8
Payload (Passengers)	35 - 70
Fuel Efficiency (Passenger miles per lb of fuel)	Fall-out

Table 1 N+2 Experimental Validation Program Goals

In Phase I, the main objective was to validate the sonic-boom signature and the cruise efficiency of a low-boom aircraft configuration. The configuration had to meet the sonic-boom goals, and its ground signature had to have front and aft sonic-boom signature shaping. Also, the low-boom configuration had to be representative of an N+2 class supersonic airliner. Phase I was broken down into the following major elements.

1. Develop a low-boom concept that meets project objectives
2. Assess sonic boom and supersonic cruise performance
3. Fabricate a modular sonic-boom wind-tunnel model
4. Fabricate a modular supersonic cruise performance wind-tunnel model
5. Conduct a sonic-boom wind-tunnel test
6. Conduct a supersonic cruise performance wind-tunnel test
7. Validate analysis/design with measured test data

In Phase II, the main focus is on propulsion integration and its effect on sonic-boom and performance. Here, the objective is to determine the effect of nacelle and nozzle shaping on the sonic-boom and efficiency. This includes the investigation of alternate N+2 propulsion integration scenarios for inlet and plume effects on sonic boom. Based on the investigation, a preferred propulsion integration scenario will be selected. Once a new propulsion arrangement is determined, the inlet and nozzle will be designed and optimized. This design will have good performance including high pressure recovery, low distortion, and minimized impact on sonic boom. Phase II will also incorporate the lessons learned from Phase I and re-optimize the complete configuration for sonic-boom and efficiency. A secondary objective for Phase II is to investigate the sonic-boom test technique challenges discovered during the Phase I validation testing. In Phase I, the uncertainty of the measured signature was on the order of the magnitude of the near-field signature that was measured. This made it difficult to validate the concept signatures with CFD. Three wind-tunnel tests (a parametric test and two exploratory tests) have been conducted to refine the near-field pressure measurement techniques and determine the best facilities to conduct validation testing in Phase II. Phase II has been broken down into the following major elements.

1. Develop a preferred propulsion integration scenario
2. Design a high performing inlet with low-sonic-boom characteristics
3. Integrate the inlet and design a low-boom concept that meets project objectives
4. Assess inlet performance, sonic boom and supersonic cruise performance
5. Fabricate a modular sonic-boom wind-tunnel model
6. Fabricate a modular supersonic cruise performance wind-tunnel model
7. Fabricate a propulsion effects model
8. Conduct exploratory wind-tunnel tests on Phase I models
9. Conduct a propulsion validation sonic-boom wind-tunnel test
10. Conduct a supersonic cruise performance and propulsion effects wind-tunnel test
11. Validate analysis/designs with measured test data

The focus of the remainder of the paper is the validation of the Phase I low-boom design using wind-tunnel data acquired in Phases I and II. The Phase II propulsion validation work is in progress and will be discussed at a later date.

III. Low-Boom Design

CFD-based shape optimization methods were utilized on the Phase I project to arrive at a concept that met the aggressive sonic-boom shaping and noise metric requirements for the project. The starting seed concept for the design work was the 765-076E configuration shown in Figure 1. That starting seed geometry was not considered low-boom, as its perceived loudness was 91.5 PLdB, but it had some ground signature shaping characteristics. Its front shock was a flat-top and the aft signature had some flat signature features too. The initial pressure rise was 0.7 psf and the aft pressure recovery was ~ 0.8 psf. It was believed that this configuration could be improved to meet the sonic-boom and performance goals of the program.

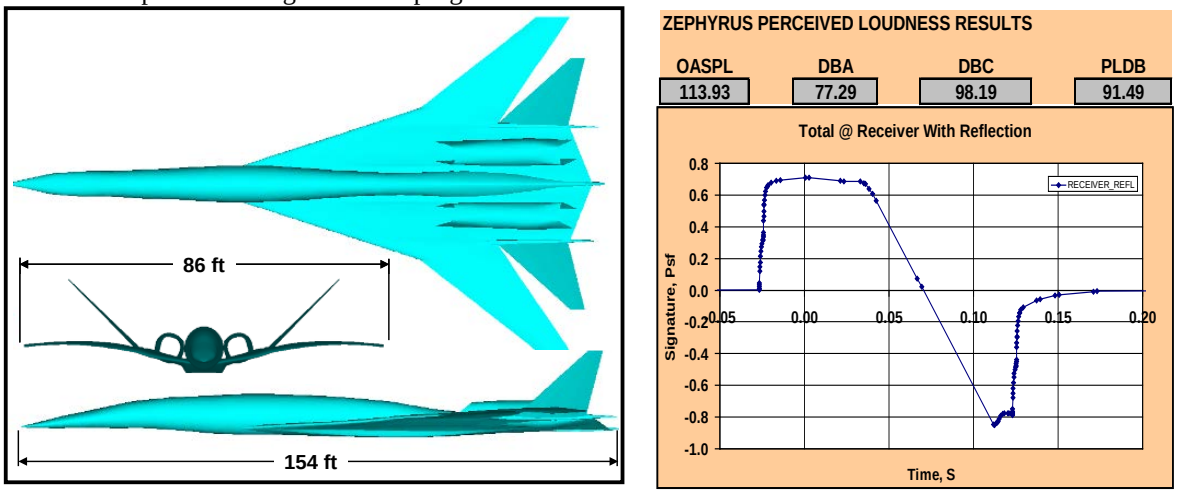

Figure 1 A Shaped Signature Seed Geometry (N+2 System Study Concept) was Selected as the Starting Point for Low-Boom Optimization

The under-track design target selected to meet the program goals is shown in Figure 2. The perceived loudness for this design target is less than 77 PLdB. The target signature was much more stringent than the goal of 85 PLdB to allow robustness at off-design and off-track conditions and to leave some margin for atmospheric turbulence effects. This target has aggressive ground signature shaping with a sine-wave / polynomial ramp-like front signature and a flat-top aft signature. It has a ~ 0.2 psf "setting" shock in the front and a 0.35 psf terminal shock. The aft signature has ~ 100 ms of 0.65 psf flat-top which transitions to a ramp at the end. The flight conditions for the design were a Mach number of 1.8 at the beginning of cruise (i.e., weight of 162,000 lbs at an altitude of 49,000 ft).

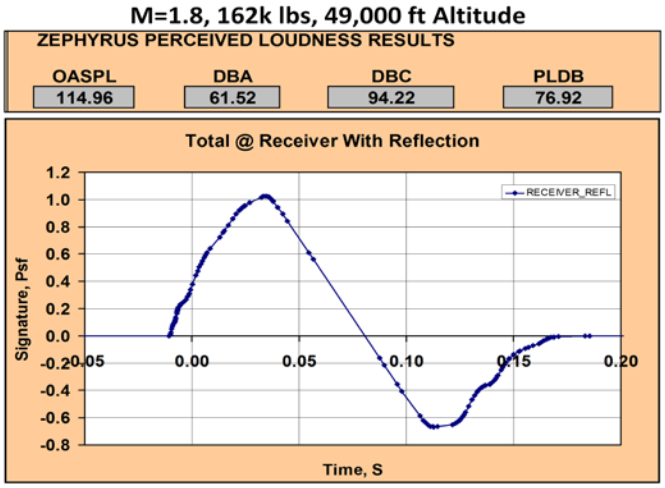

Figure 2 An Aggressive Shaped Signature Design Target was Selected for the Phase I Concept

The design was conducted on the full-scale flight vehicle in Phase I, but during manufacturing of the validation wind-tunnel models it was found that some of the features in the design did not scale to the wind-tunnel size. Adjustments were made to the wind-tunnel model design and the configuration was re-analyzed to ensure that the boom shaping and sound levels were retained. Based on this experience it was determined that the Phase II designs would be conducted on the wind-tunnel model OML, thus alleviating the need to re-analyze and re-design features that do not scale well.

A. Methodology

A design of experiments approach was used to optimize the off-body pressure signature and the airplane performance. The process consists of setting up a series of geometric design variables, using CFD to predict the off-body pressure signature at 3 body lengths, and optimizing to find better design variable settings. The inviscid CFD analysis was performed using the OVERFLOW solver [10]. The Boeing-developed optimization tool MDOPT [11] was used to drive the design of experiments optimization process. The optimization process illustrated in Figure 3 consists of the following steps:

1. Set up design variables to perturb the geometry
2. Generate an orthogonal array of sites with combinations of the design variables
3. For each site,
   a. Run a CFD flow solution with the perturbed geometry
   b. Compute the objective and constraints as a function of the off-body signature and the airplane performance
4. Generate a surrogate model of the objective and constraints as functions of the design variables
5. Perform model-based optimization on the surrogate model to find new good sites predicted by the model
6. Analyze the model-based optimization sites
7. Repeat steps 5 and 6

Through this optimization process, flow solutions were computed for thousands of different geometries. The final design was selected from the most-promising sites from the optimization based on trading the objectives and constraints as well as geometric features.

The Phase I design consisted of a series of preliminary design steps, taken to produce a seed geometry that has the potential to achieve the desired PLdB at the ground and meet the performance requirements, followed by detailed optimization. For this stage of the optimization, the PLdB was required to be less than 85 and the inviscid drag coefficient target at Mach number of 1.8 and CL of 0.10 was 0.0079. A history of these two objectives through the optimization process is shown in the bottom two images in Figure 4. In the figure, the upper left plot tracks the near-field pressure signature, the plot in the upper right-hand corner tracks the propagated ground signature, the plot in the lower left-hand corner tracks the cruise pressure drag and the plot in the lower right-hand corner tracks the

ground PLdB. The optimized design represents the geometry which meets the signature requirement and is close to meeting the drag target. Figure 5 shows the surface pressures and the centerline pressure distribution for the optimized configuration. Figure 6 shows the general arrangement for the Phase I low-boom concept.

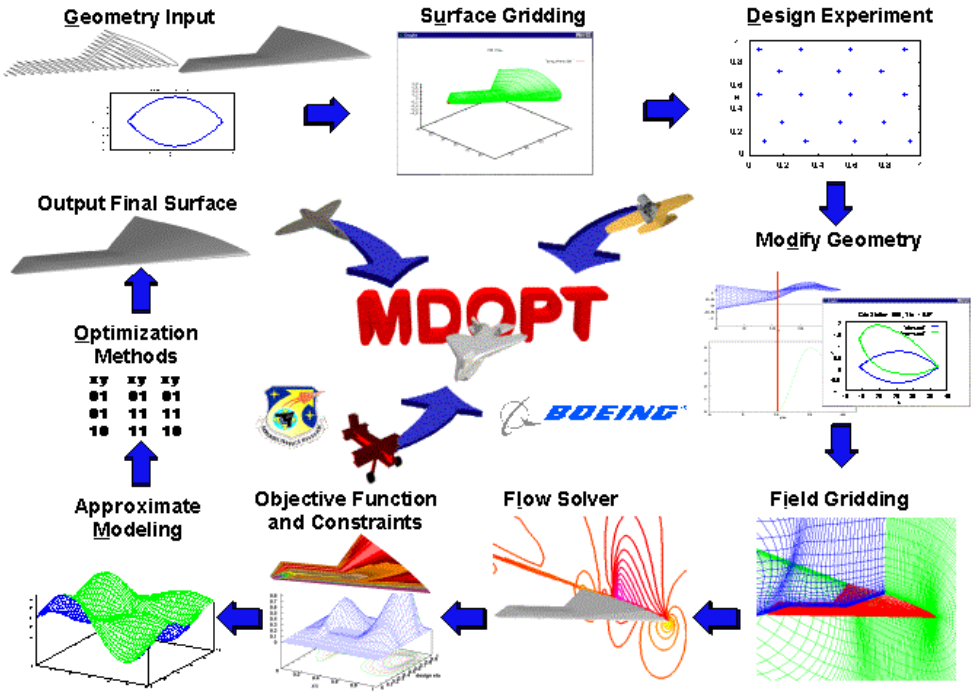

Figure 3 An Integrated Design-of-Experiments Approach (MDOPT) was Utilized to Optimize the Low-Boom Concept

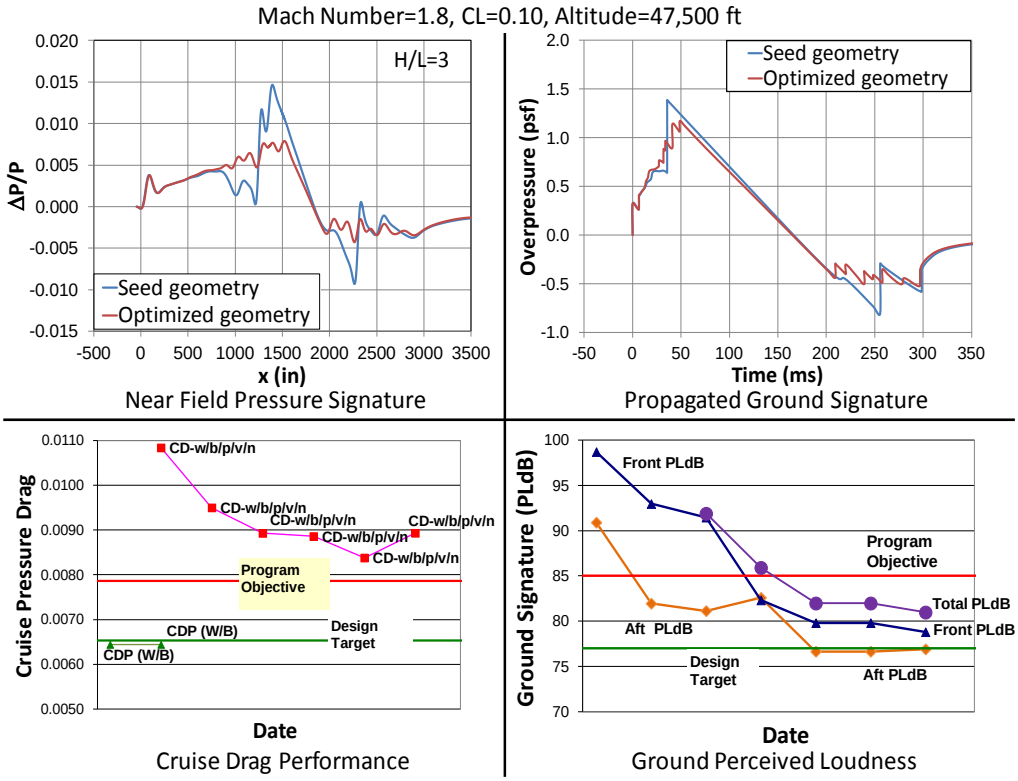

Figure 4 Pressure Drag, Near-field Signature, Ground Signature, and PLdB were Utilized to Track Optimization Progress

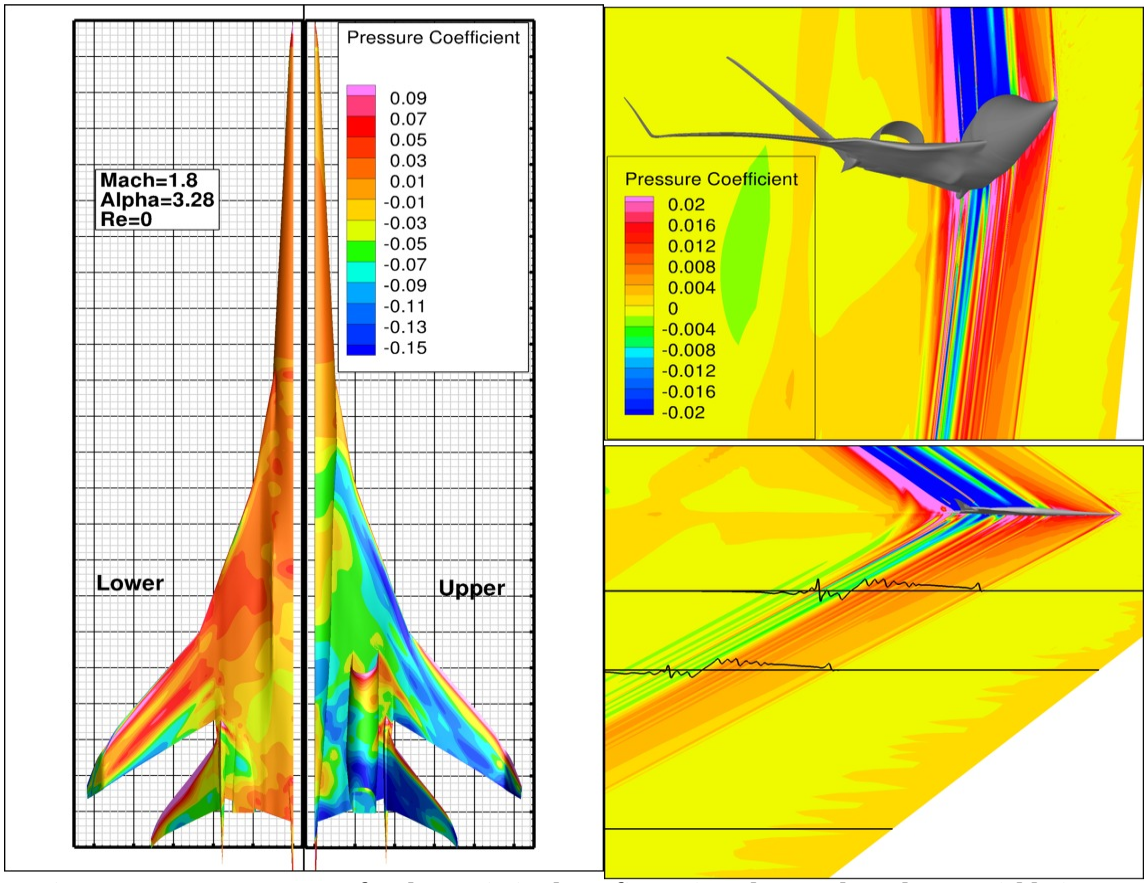

Figure 5 Pressure Contours for the Optimized Configuration Show a Shaped Near-Field Signature

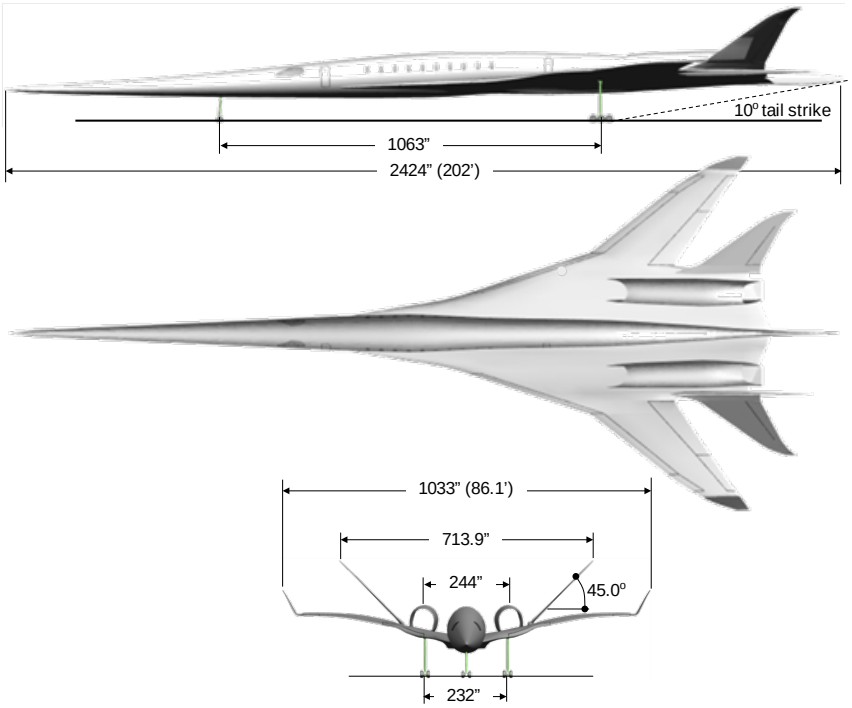

Figure 6 Optimization Resulted in the Low-Boom Concept General Arrangement

The sonic-boom qualities and the aerodynamic performance of the resulting low-boom design were verified by analysis as described below.

B. Sonic Boom Analysis

In Figure 7, the detailed sonic boom analysis using OVERFLOW and Zephyrus is shown for two Mach numbers, 1.8 (design) and 1.6 (off-design). In the upper portion of the curve, the near-field pressure distributions are shown for several H/L locations. Essentially, stable near-field distributions are achieved for H/L locations of 2.0 or more. When an H/L is not shown in a sonic boom figure, it is assumed that H/L = 3. In the lower half of Figure 7, the ground signature is shown for both Mach = 1.8 and Mach = 1.6 and for the same H/L variations. For H/L values of 2.0 or more, shaped fore and aft ground signatures are achieved for the low-boom concept at both Mach numbers. In addition, all ground signatures are below the 85 PLdB goal, with the lowest one at ~81 PLdB.

The low-boom concept was also examined at off-design CLs at each Mach number to determine whether signature-shaping persists to the ground and the perceived loudness is still below the 85 PLdB goal. Figure 8 shows this for Mach = 1.6 and 1.8, at H/L = 3 for three different CL values. Again, both the near-field and ground signatures are shown in the figure. From Figure 9, many off-design CLs continue to show fore and aft shaping. For a CL = 0.08 at Mach = 1.8, however, the aft signature starts to approach an N-wave, and ground-perceived loudness is above the 85 PLdB goal. All Mach = 1.6 cases show shaped signatures for all CLs considered, and ground-perceived loudness essentially meets the 85 PLdB goal.

Finally, Figure 9 shows the variation of the sonic boom signature with off-track location for Mach 1.6 and 1.8 at H/L = 3. The near-field and ground signatures are portrayed in the same way as the previous figures. The low-boom concept retains signature-shaping and ground-perceived loudness, to some extent, when moving away from under-track. At Mach = 1.8, the shaping persists to approximately 15 deg off-track. The ground-perceived loudness also is maintained below 85 PLdB up to 10 deg off-track. At Mach = 1.6, the shaping and ground-perceived loudness remain at the goal or lower for up to 30 deg off-track. This was a favorably robust result, given that the concept was designed at the Mach = 1.8 condition.

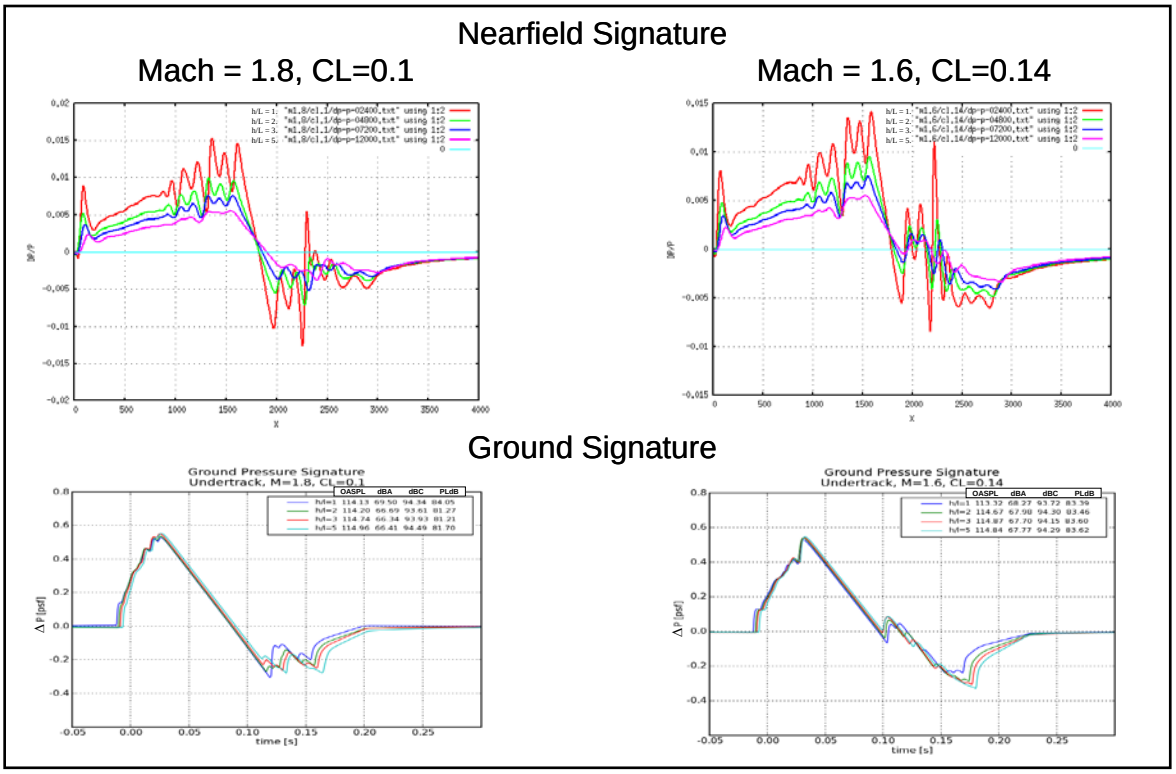

Figure 7 The Low-Boom Concept Has Robust Sonic Boom Characteristics at Multiple Mach Numbers

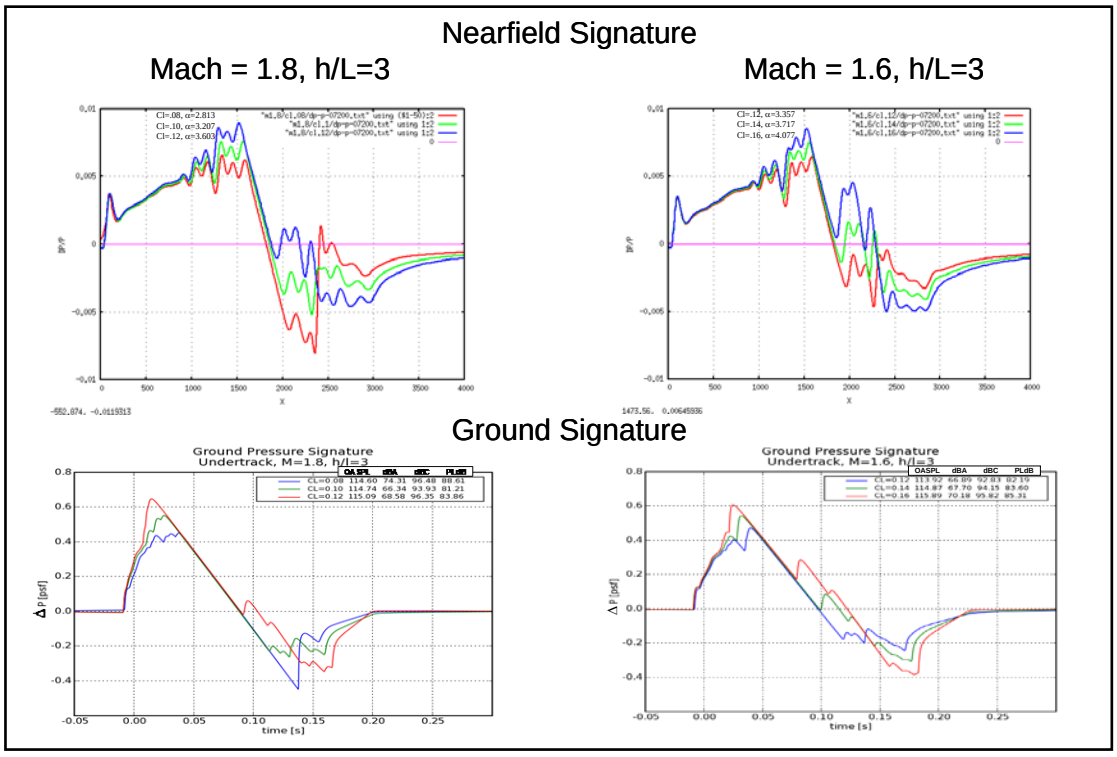

Figure 8 Low-Boom Concept Signature Characteristics at Off-Design CLs

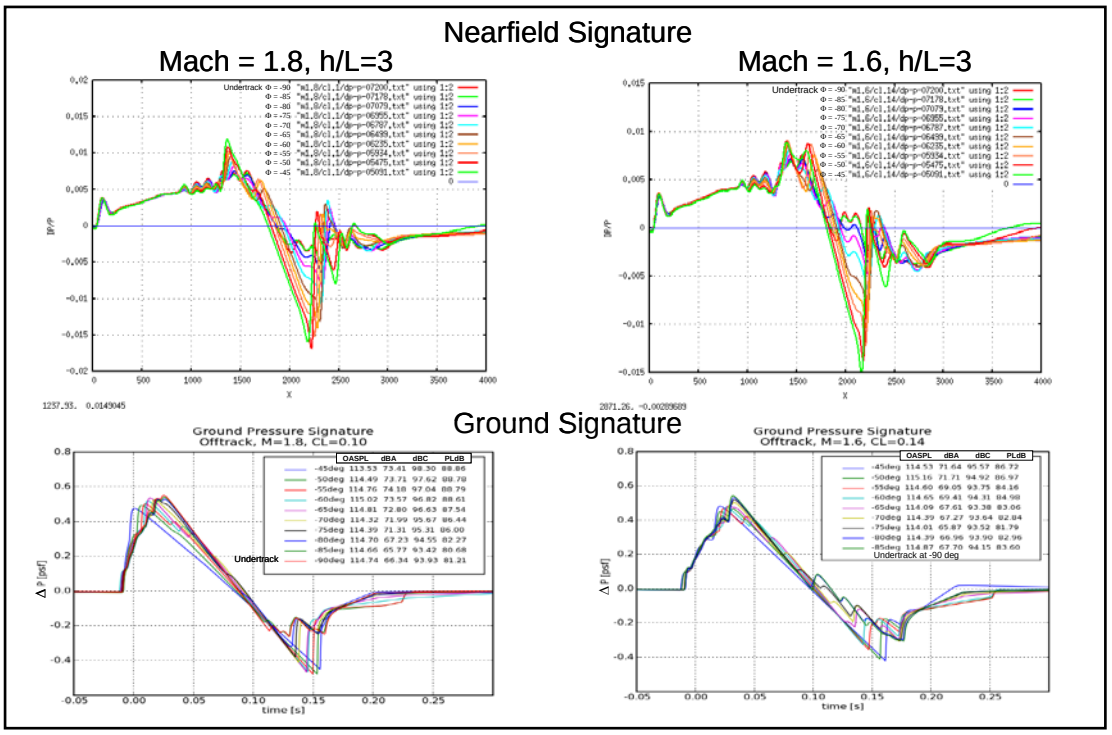

Figure 9 The Low-Boom Concept Has Robust Signature Characteristics at Off-Track Locations

C. Cruise Aerodynamic Analysis

An aerodynamic analysis was conducted for the low-boom concept at the Mach 1.6 and 1.8 cruise condition. Figure 10 summarizes the Navier-Stokes results. The left plot contains the drag polar (CL versus CD) and the right plot contains the pitching moment (CM versus CL). The drag polar contains the inviscid drag for the concept. During the optimization, the planform and length were held constant, so the viscous drag essentially remained fixed. Thus, pressure drag was the variable that was utilized to determine whether the optimized low-boom concept achieved the 765-076E configuration goal level of performance. The 765-076E configuration goal pressure drag is 79 counts. The low-boom concept pressure drag at the Mach 1.8 design condition is ~86 counts, which is 7 counts above the project goal value. However, at the Mach 1.6 design condition the low-boom concept pressure drag meets the project goal. Furthermore, with a technology projection to 2025 (and further optimization), the Mach 1.8 performance can exceed the goal of matching the 765-076E pressure drag levels. Based on this analysis and reasoning, the low-boom concept was deemed sufficient for experimental validation testing.

The pitching moment in Figure 10 indicates a very statically stable configuration as a result of the lift generated on the aft-deck of the configuration. Since this results in undesirable flying qualities for the aircraft, a second concept design was developed that worked both the drag and pitching moment while trying to constrain the achieved sonic-boom levels from the first design. The second optimized configuration successfully achieved lower drag and improved pitching moment. Both concepts were validated through wind-tunnel testing as described in Section IV.

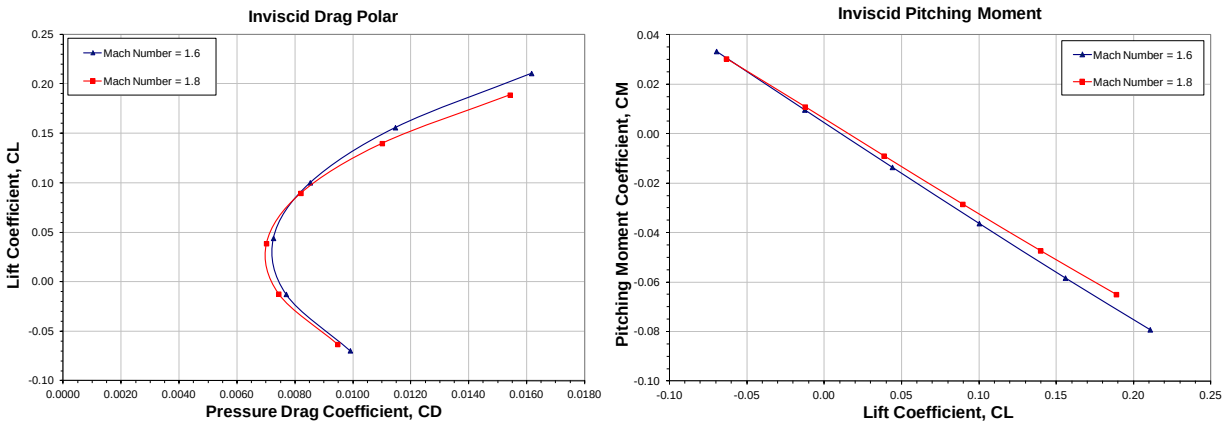

Figure 10 Cruise Aerodynamic Analysis Indicates a Low-Boom Configuration Worthy of Validation

IV. Validation Wind-Tunnel Testing

Several validation wind-tunnel tests have been conducted in Phase I and II of the project. Initially, it was thought that only one sonic-boom and performance wind-tunnel test would be required to validate the low-boom concept in each phase. However, after the first two wind-tunnel tests it was realized that the test techniques needed additional development to achieve the desired validation results. These tests were the first time that a truly low-boom configuration with both front and aft signature shaping were tested in a wind tunnel. Measured sonic-boom signature levels were small, so instrumentation and wind-tunnel distortion affects became important. This section describes the wind-tunnel models, instrumentation, and tests conducted in Phase I and II that were utilized to validate the low-boom concept.

A. Validation Wind-Tunnel Model Design

The experimental validation program was centered on two models: a large model primarily for performance validations, with some capability for boom testing; and a smaller 1/3-size version of the performance model, primarily for boom measurements. In addition, several extra small parts for each model were fabricated to obtain sensitivities on boom and drag to verify that the CFD validation could cover incremental effects.

For the large model, two additional outboard wings, an alternate nacelle, and an alternate V-tail were designed. One of the alternate outboard wings, along with the V-tail, was a product of changing the wing and tail to minimize drag. The alternate nacelle had a 2D inlet.

	Boom Model 1	Boom Model 2
Objective	Lowest Sonic-Boom	Low Drag while maintaining Low-Boom
Mach	1.8	1.6
Lift Coefficient	0.104	0.140
Pitching Moment	No Constraint	Constrained to -0.02

Table 2 Design Criteria for Sonic Boom Models

For the small boom model, a different approach was taken. Instead of fabricating a series of alternate parts (e.g., a nose, gear fairing, nacelle, and tail), a complete alternate design was chosen. To ensure that the second optimization produced a geometry that would be significantly different from that produced by the first optimization, design conditions were changed from Mach 1.8 (CL = 0.1039) to Mach 1.6 (CL = 0.14). In addition, the weighting of objectives was adjusted, so that the focus was more on drag and pitching moment than the near-field signature shape. Table 2 compares the design criteria of Boom Models 1 and 2.

The three wind-tunnel models were designed and fabricated by Tri Models Inc. The two sonic-boom models are 0.65% scale representations of the low-boom concept. The performance model is a 1.79% representation of the low-boom concept. They are shown in Figure 11. The sonic-boom wind-tunnel models are supported by an upper-swept strut. The performance model is sting mounted. The upper-swept strut allows the installation of an internal balance, so that the model loads can be measured during the test. Two upper-swept struts were fabricated. The first one is longer to allow a greater extent of the aft signature to be measured without interference. The second one is shorter and was fabricated in case there were model dynamics with the larger strut. A set of large fins were also fabricated to use with the struts to dampen any aeroelastic effects if they are present.

Modular (~.0065 Scale) QEVC Small Boom Models

Modular (~.0179 Scale) QEVC Large Force Model

Figure 11 In Phase I an Extensive Set of Modular Validation Wind-Tunnel Models were Built

In addition to the low-boom models, there were three axisymmetric models (AS1, AS2, and AS3) that were fabricated to calibrate the near-field pressure measurement instrumentations utilized on the tests. These Body-Of-Revolution (BOR) models represent SEEB equivalent area distributions with well known near-field pressure distributions. Thus, they are ideal for assessing the quality and uncertainty of the pressure measurement instrumentation. The AS2 model represents the equivalent area distribution for the Phase I low-boom concept. The AS3 model represents 2X the equivalent area distribution of the Phase I low-boom concept. The AS1 model represents a SEEB body that has been tested prior to the N+2 Experimental Validation program. Figure 12 contains a picture of the AS2 BOR model.

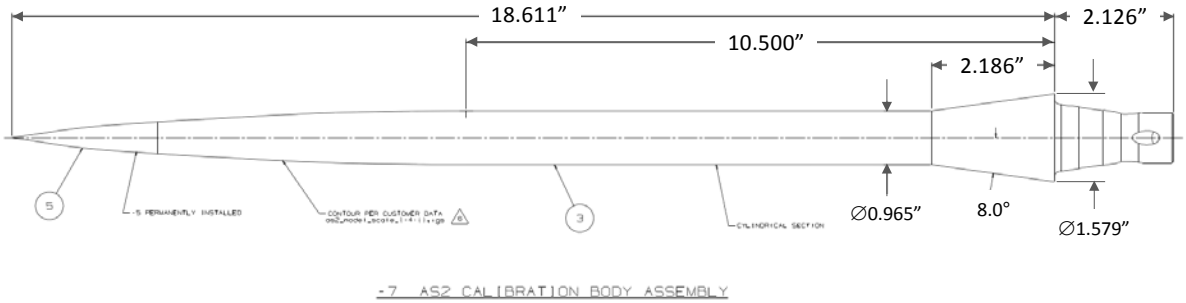

Figure 12 AS2 BOR was Utilized to Calibrate the Pressure Measurement Instrumentation

B. Validation Test Instrumentation

Since the test objectives were to validate the sonic-boom and performance of the low-boom concept, two main types of instrumentation were utilized, a 6-component strain-gage balance and a pressure measurement rail. The strain-gage balance was utilized to measure the 6-components of force and moment on the model. This way the CFD results can be correlated and matched with the exact test conditions and forces measured. The force and moment balance was internally mounted in the performance model. For the BOR models, it was mounted internal to the balance adapter housing. The sonic-boom models had it mounted in the balance adapter housing of the aft swept strut.

The pressure rail measures the model off-body near-field signature. It is mounted either on the wind-tunnel wall, floor, or ceiling and the model is mounted a specific distance away from it. Two pressure measurement rails were utilized in the sonic-boom testing, a 14" tall blade rail and a 2"tall flat-top rail. Each rail has its unique advantages and disadvantages in terms of the interference and distortions it causes on the measured pressure results. The 14" blade rail provides a reflection factor of 1 on the measured pressure signature, whereas the 2" flat-top rail provides a larger reflection factor of 1.3. This is because the blade rail has a very small radius top while the 2" rail has a relatively wide flat-top. The reflection factor off the top of the rail approaches 1.9 as the width of the top becomes larger. Another flow interference/distortion that rails are affected by is the reflection of the incoming signal off of the wind-tunnel wall to which the pressure rail is mounted. The taller the rail, the farther downstream the influence of this reflection is measured. The 2" rail distorts the measurement on the front side of all of the models, whereas the 14" tall rail has no wall reflection effect for the small sonic-boom models. Both pressure measurement rails can provide good results with the appropriate corrections. However, the 14" rail became the predominant measurement rail in the Phase I and II validation testing, because it had the simplest and least number of corrections required to obtain good results. A diagram for the 14" pressure rail is shown in Figure 13. The 2" pressure rail is shown in Figure 14.

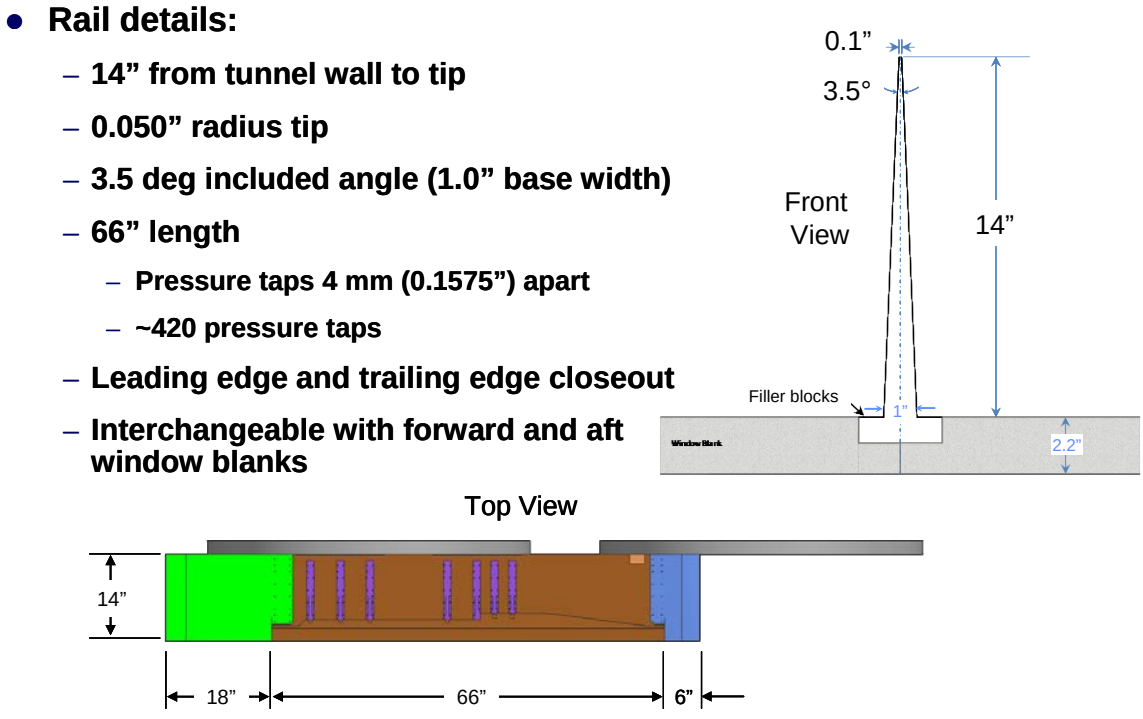

Figure 13 The 14" Pressure Measurement "Blade Rail" was the Predominate Rail Used on the Project

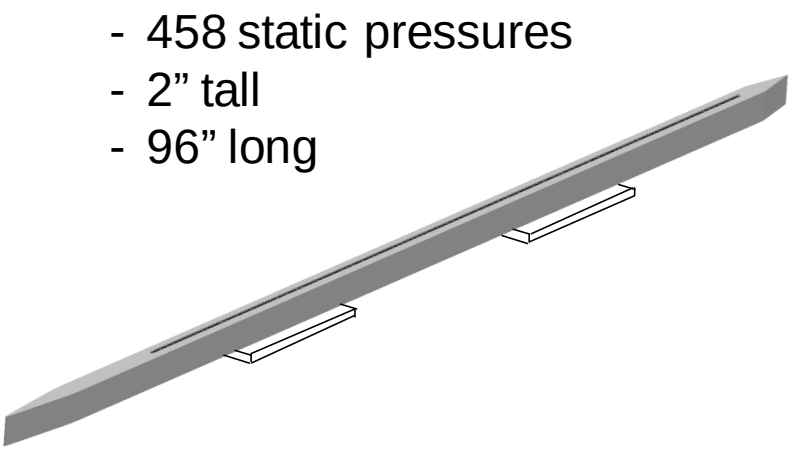

Figure 14 Boeing 2" Pressure Measurement Rail Allows the Largest Sonic-Boom Models to be Tested

C. Wind-Tunnel Tests

In Phase I and II, five wind-tunnel tests were conducted using the Phase I wind-tunnel models. Each wind-tunnel test added something to the overall validation of the low-boom concept. Two validation wind-tunnel tests were conducted in Phase I, a rail validation test and the low-boom concept validation test. The rail validation test was conducted to determine the quality and validity of data gathered using a 14” tall blade pressure measurement rail. Boeing was responsible for the model design and fabrication of this new pressure rail. The low-boom validation test was conducted to validate the sonic-boom and performance of the Phase I low-boom concept.

Three wind-tunnel tests have been conducted in Phase II. They include a parametric wind-tunnel test and two exploratory wind-tunnel tests. The parametric test was conducted by NASA to examine test techniques for accurately measuring the near-field pressure signature. The exploratory tests were conducted at the NASA Ames 11’ and NASA Glenn 8’ x 6’ wind tunnels to examine sonic-boom measurement capabilities and uncertainties in alternate facilities. The exploratory tests were also conducted to determine the best test facility for conducting the Boeing Phase II low-boom concept validation. The Boeing Phase II validation testing involves inlet performance testing which requires an expanded Mach range over what can be achieved at the NASA Ames 9’ x 7’ wind tunnel. Therefore, it was important to see how the expanded Mach range facilities could handle both the inlet performance and sonic-boom testing.

1. Rail Validation Test

The 14” rail validation test was conducted at the NASA Ames 9’ x 7’ wind tunnel in the fall of 2010. The test was part of a Lockheed Martin test series for their N+2 Experimental Validation effort. Boeing’s participation was only during the first part of the test where the new 14” pressure rail was being checked out and validated. Three models were utilized for the new pressure rail validation. They include the Lockheed SEEB-ALR axisymmetric model, NASA Ames low-boom wing-tail model (LBWT), and Lockheed N+2 optimum signature axisymmetric model (OptSig). Figure 15 shows the LBWT model installed in the Ames 9’ x 7’ wind tunnel with the 14” blade

Figure 15 14" Pressure Measurement Rail Installed in the NASA Ames 9' x 7' wind tunnel with NASA LBWT Model

rail. A diagram that details the wind-tunnel support hardware, model installation, and blade pressure rail location is shown in Figure 16. The installation results in a long flexible configuration comprised of the model, Ames sting, LM sleeve, ram, linear actuator, roll mechanism, and SR-57 primary strut adapter. This setup allows the model to be located in a large range of X and Z locations in the wind tunnel. It also allows the model to be rolled to acquire off-azimuth near-field pressures.

Rail validation data was gathered at Mach numbers from 1.6 to 2.0, heights above the rail from ~10.6 inches to ~40.7 inches, and Ram positions from 0 to 24 inches. Data was also acquired for the blade pressure rail located in both the forward and aft locations in the wind tunnel. Reference runs were taken for the model located in an up and away location (height greater than 61 inches and Ram at the 0 inch position) from the rail where the model signature did not influence the pressure rail measurements. These reference runs were subtracted from the data runs to remove the clean-tunnel influence of the pressure rail on the results. At each model position, rail pressure data was taken over a time interval from which the final pressure data is grouped into different averaging subintervals (i.e., a total 60 second time interval at a single model position could result in a data output of averages of every 1s, 2s, 5s, 10s, 20s, etc). For most data reduction, the average of the interval from 5s – 10s was used, and the total data taking interval limited to 16s. All of the tests used similar installations and data reductions as described above.

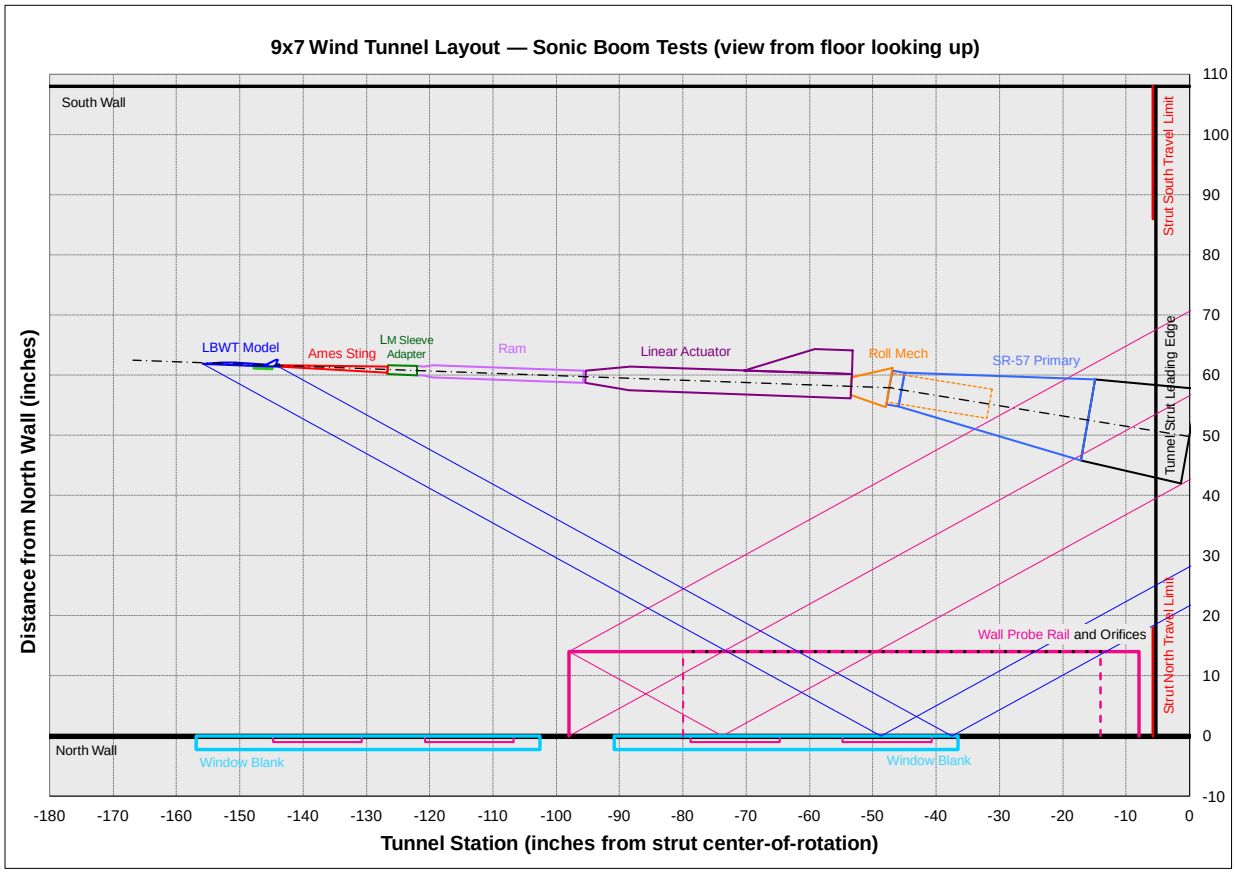

Figure 16 NASA Ames 9' x 7' Layout for the 14" Rail Validation Test

2. Low-Boom Validation Test

Phase I low-boom validation testing was conducted at the NASA Ames 9' x 7' wind tunnel. The Boeing 2" pressure measurement rail was utilized to obtain the near-field pressure distribution for each model. Details of this pressure rail are shown in the diagram contained in Figure 14. It is 2" tall by 96" long and contains 458 pressure orifices. Five wind tunnel models were tested during the validation test. They include two small sonic-boom models (BM1 and BM2), a performance model (PM1), and three bodies-of-revolution (AS1, AS2, and AS3). Photographs of the PM1 and BM1 models installed in the Ames 9' x 7' wind tunnel are shown in Figure 18. The total configurations tested are shown in Figure 19. The body-of-revolution models were utilized to assess the

Figure 17 Boeing 2" Pressure Measurement Rail Installed in the NASA Ames 9' x 7' Wind Tunnel with the Boeing Body-of-Revolution

accuracy of the 2" pressure measurement rail (see Fig. 17). Both the sonic-boom and performance models were tested parametrically in order to determine the effect of each component on the near-field pressure signature. Configuration testing started with the wing/body and then added components until the complete configuration was tested. Test conditions include Mach numbers of 1.6 and 1.8, nose height from the pressure rail of 24 – 36 inches and 54-66 inches for the sonic-boom (BM1 and BM2) models, and nose height from the pressure rail of 54-66 inches for the PM1 model. The linear actuator was not used in this test setup. Figure 20 contains the model installation layout for the low-boom validation test. During the force and moment testing, the PM1 model pitch polar data was gathered for angles-of-attack from +1 to +6.25 degrees in 0.25 degree increments. The BM1 and BM2 model were tested at 3.5 and 4 degrees angles-of-attack.

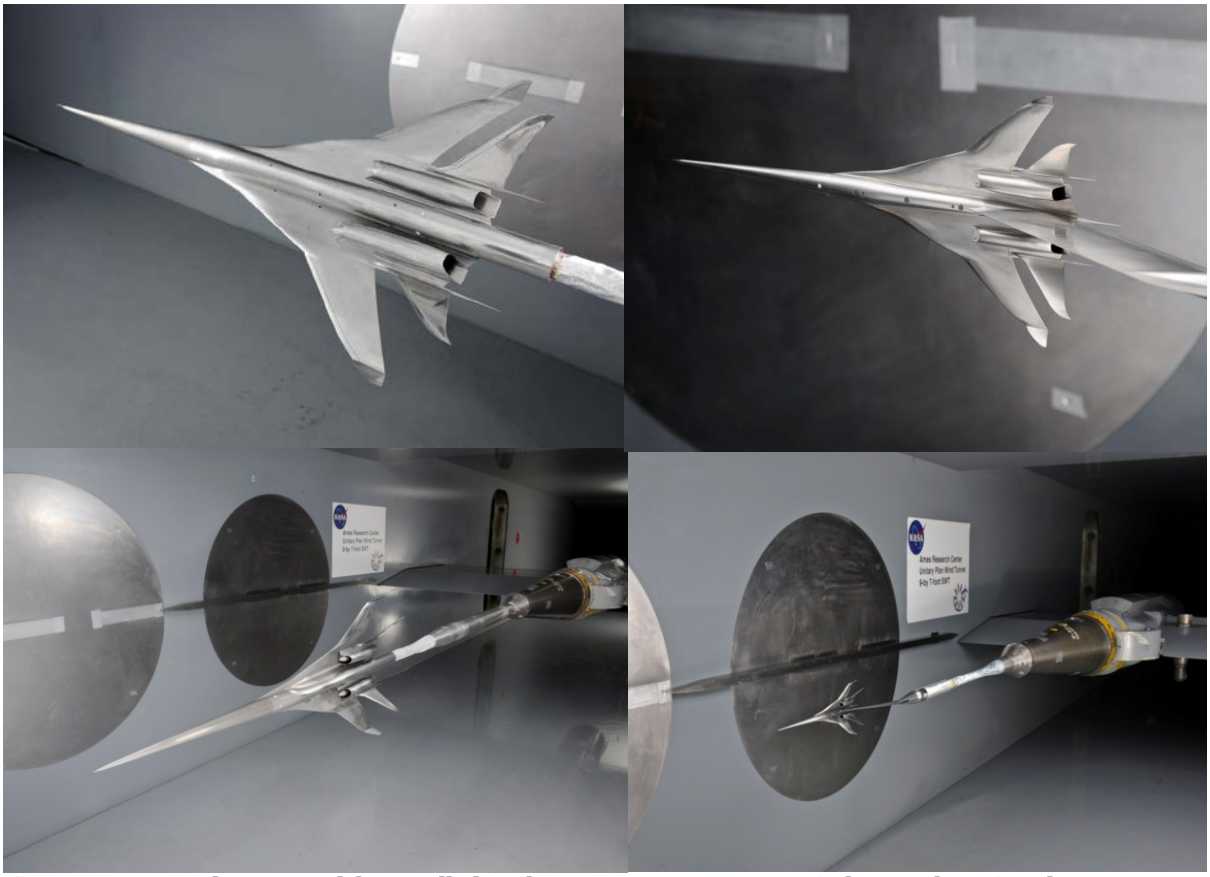

Figure 18 PM1 and BM1 Models Installed in the NASA Ames 9' x 7' Wind Tunnel During the Low-Boom Validation Test

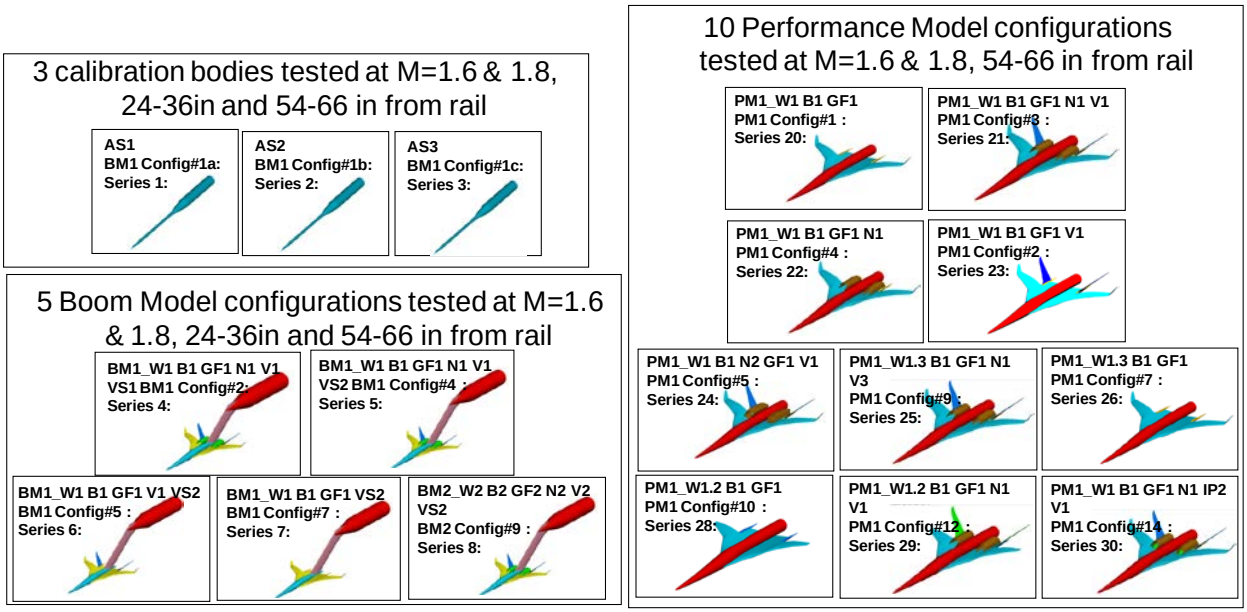

Figure 19 Eighteen Configurations were Tested in the Boeing Phase I Validation Wind Tunnel Test to Determine Their Effect on the Near-field Pressure Signature

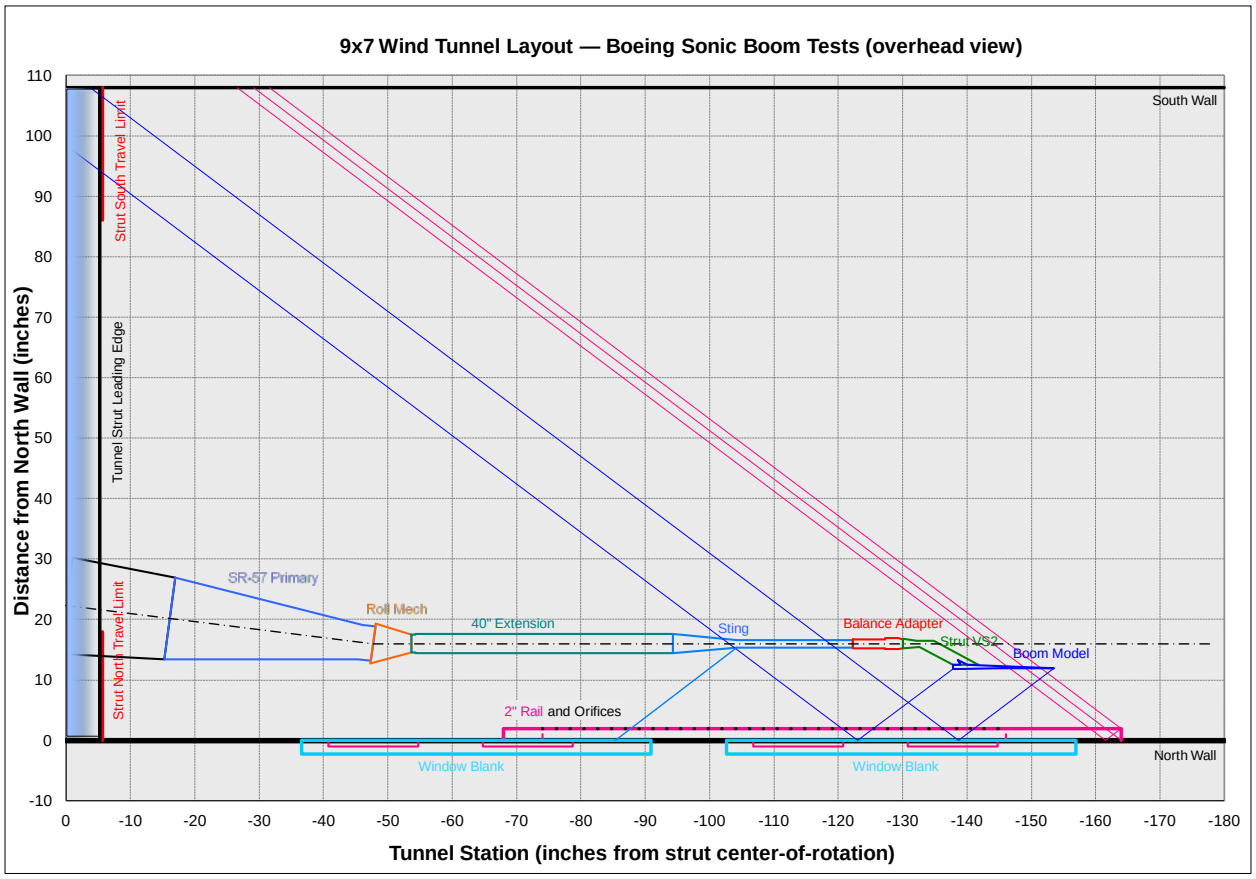

Figure 20 NASA Ames 9' x 7' Layout for the Low-Boom Validation Test

3. Parametric Test

The parametric test was conducted by NASA in the spring of 2012 at the NASA Ames 9' x 7' wind tunnel. The objective of the test was to determine the best test techniques to measure the near-field pressure signature. Previous sonic-boom tests using pressure measurement rails showed a significant amount of uncertainty in the results compared with CFD. The comparison was not consistent based on spatial and temporal points in the wind tunnel. This was a big issue, because the signal strength of the low-boom concept was the same order of magnitude as the observed uncertainty in the previous wind-tunnel tests.

Two pressure measurement rails were examined during the test, the Boeing 2" pressure rail and the NASA 14" blade pressure rail. The Boeing small sonic boom model and AS2 body-of-revolution model were tested along with the Lockheed Martin low-boom concept and body-of- revolution. Spatial and Temporal averaging techniques were examined during the test along with the effect of humidity. Both X-sweep and Z-sweep spatial averaging runs were conducted. See References 12 and 13 for additional details.

Spatial averaging was conducted by acquiring data at several positions in the fore-aft direction for an 'X-sweep', or in the vertical direction for a 'Z-sweep'. Most sweeps were performed by moving the model by the equivalent of 4 rail pressure ports for a total of about 25 model positions. This results in about 8 inches of linear actuator motion for X-sweeps, or about 8 vertical inches for Z-sweeps (depending on Mach number).

The test conditions for the parametric test were Mach numbers of 1.6 and 1.8, heights of 30 inches and 60 inches, and Ram positions from 0 to 24 inches. Since spatial averaging was conducted during this test the linear actuator and Ram were added to the model installation. The NASA Ames 9' x 7' wind-tunnel layout for this test is shown in Figure 21.

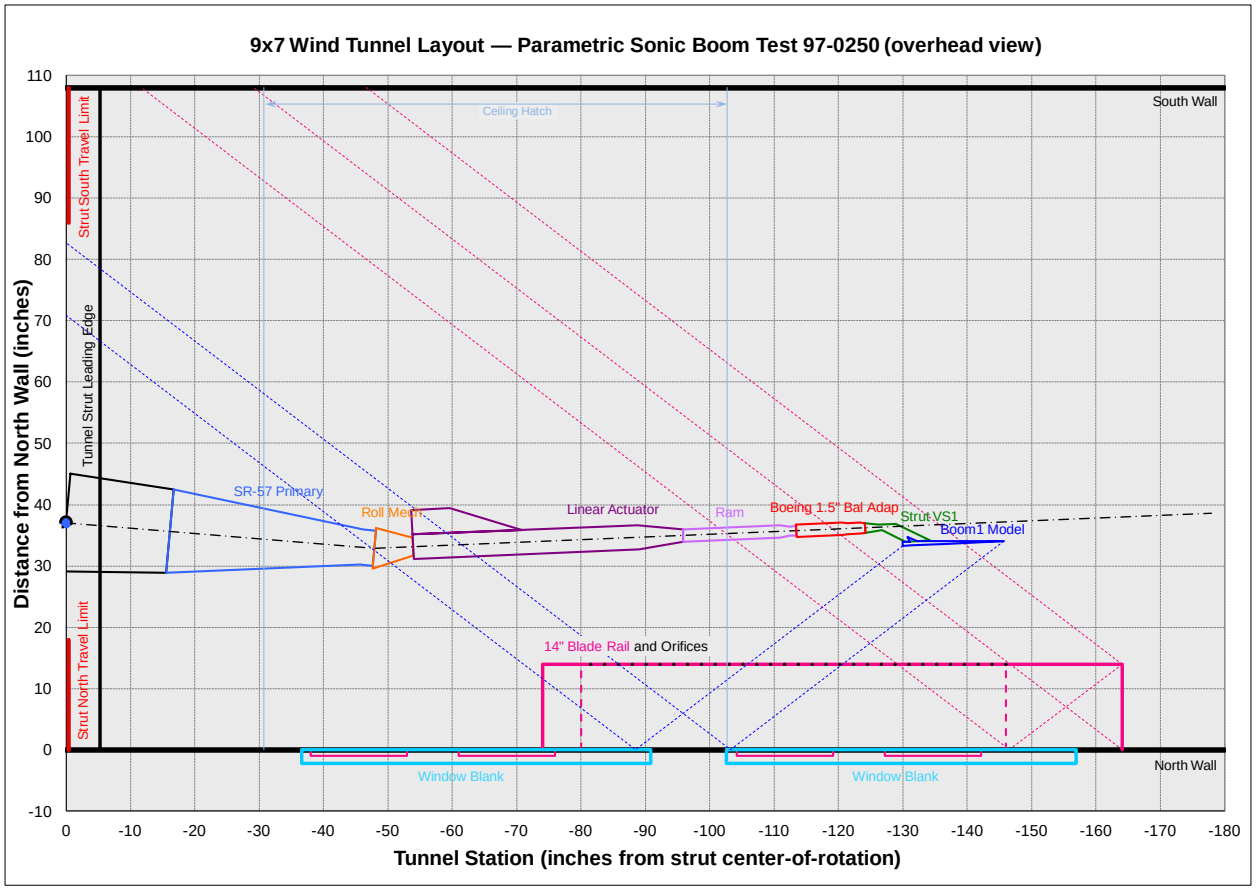

Figure 21 NASA Ames 9' x 7' Layout for the Parametric Test

4. Exploratory Wind Tunnel Testing

With the emphasis of the Phase 2 validation effort to be on propulsion integration, there was some concern that while testing at the NASA Ames 9'x7' could provide adequate sonic-boom and performance data gathering capability at the N+2 cruise conditions, it would not be able to provide the transonic conditions which would be

valuable to more completely characterize inlet performance. A series of short tests were proposed at wind-tunnel facilities that would be able to provide an expanded Mach range to cover these off-design conditions. The NASA Ames 11' and the NASA Glenn 8'x6' were proposed, with the NASA Ames 11' being considered as the complementary transonic facility to the NASA Ames 9'x7' (Table 3). As exploratory tests with a short entry (less than 1 week) and with a short preparation time (a few months), the goal was to minimize the cost and effort needed to incorporate the model hardware and pressure rail instrumentation into each tunnel while ensuring that the tested configurations would be able to provide a definitive answer as to the quality of the data gathered. Additionally, keeping in mind potential future wind-tunnel testing for a flight demonstrator, these facilities would be evaluated in terms of productivity. The results of these short tests would be used to form a recommendation as to which facility to use for the final Phase II validation test.

	NASA Ames 11'*	NASA Ames 9' x 7'*	NASA Glenn 8' x 6'**
Test Section	11 ft x 11 ft with slotted walls	9 ft x 7 ft with solid walls	8 ft x 6 ft with perforated walls (transonic section)
Tunnel Circuit	Closed Circuit	Closed Circuit	Closed Circuit***
Mach Range	0.2 – 1.5	1.54 – 2.56	0.36 – 2.0

*Test Planning Guide for High Speed Wind Tunnels, Ames Research Center
**NASA Lewis 8- By 6-Foot Supersonic Wind Tunnel User Manual
***vented to atmospheric

Table 3 Wind-Tunnel Facilities Considered for Exploratory Testing

NASA Ames 11' Test:

Some of the key issues with boom testing at the NASA Ames 11' tunnel were the rail placement and the maximum attainable Mach number. Due to the floor balance mount and floor substructure, only a relatively short area was available to mount the pressure rail. However, the available support hardware was able to position the model adequately to pick up boom signatures for the expected Mach range. The maximum achievable Mach was unknown since there would be some blockage introduced by the model which would reduce the maximum Mach capability of the tunnel.

Figure 22 PM1 Model with the 14 inch Pressure Rail in the NASA Ames 11' Wind Tunnel

Figure 22 shows the performance model installed in the NASA Ames 11' wind tunnel. The support hardware for the Ames installation included a linear actuator to provide model translation capability and a roll mechanism to provide roll capability. The layout is shown in Figure 23. Three models were tested, a body of revolution, the strut mounted BM1 model, and the sting mounted PM1 model. The Mach range covered 0.8 to the maximum achievable with angles-of-attack from -1 to +7 degrees to gather force polars. The subsonic Mach numbers were run for force data, while the supersonic Mach numbers were run for force and boom data.

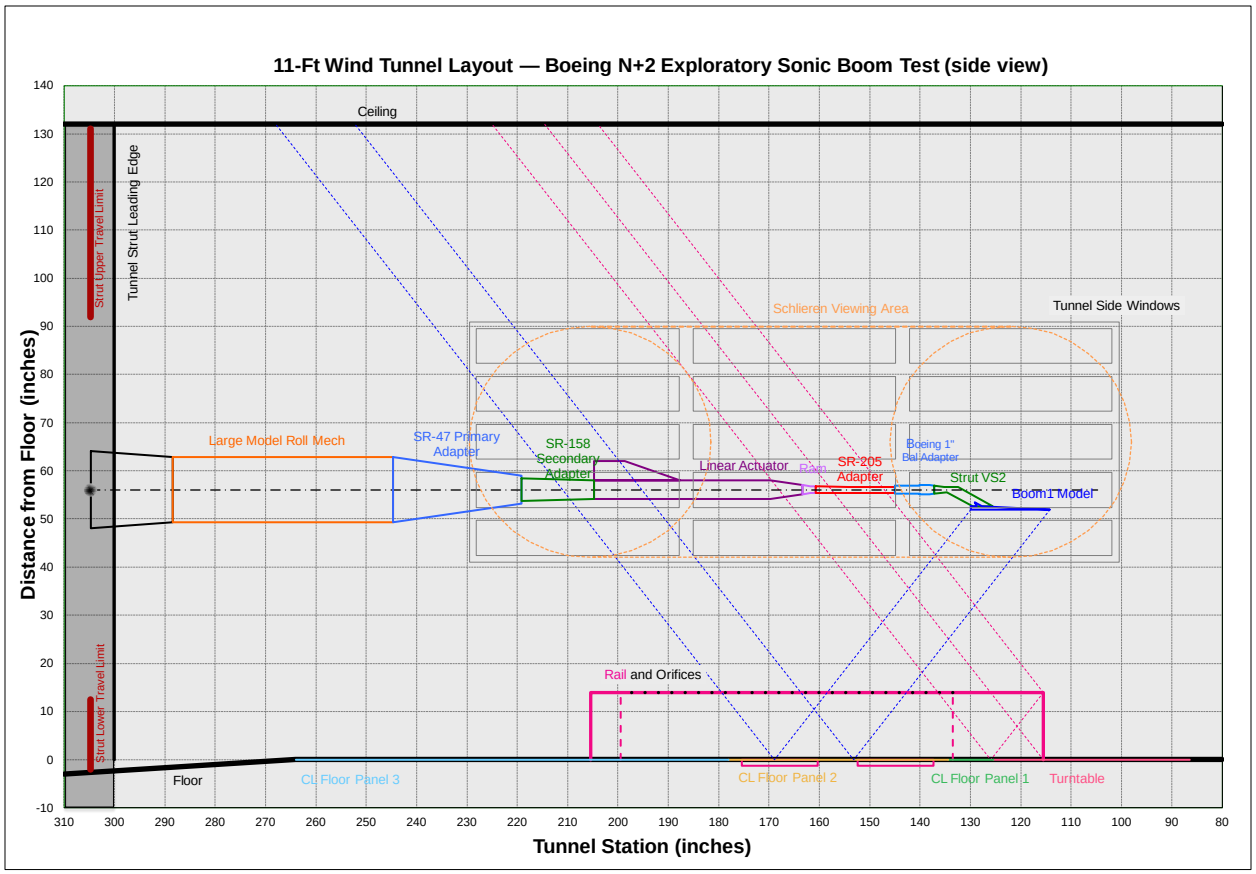

Figure 23 NASA Ames 11' Wind Tunnel Layout for the Exploratory Test

The pressure rail used for the NASA Ames11' exploratory test was the 14" blade rail discussed earlier. This rail was designed to provide an interference free boom signature for small models. Previous testing had shown that averaging multiple boom signatures acquired by translating the model in X (forward or aft), or in Z (up or down relative to the rail) can improve the signal resolution, and this same technique was used throughout the exploratory tests. A Schlieren imaging system was also used to record flow features.

NASA Glenn 8' x 6' Test:

The NASA Glenn 8'x6' wind tunnel offered the advantage of have a broad Mach range allowing boom and force data to be collected at a single facility. This extended Mach range could potentially reduce the amount of time and effort needed to run tests at multiple facilities in order to cover the required conditions.

In addition to the 14" blade pressure rail used for the NASA Ames 11' exploratory test, the 2" flat-top pressure rail was also used. The Glenn models and pressure rail were installed inverted due to the ceiling panels being the easiest to modify for the pressure rail installation. The model was mounted on a strut that protrudes out of the floor panels and provided angle-of-attack movement, however an automated roll mechanism was not used. The rail and model positioning also allowed Schlieren images to be taken of the models at their respective design cruise Mach numbers. Later in the test, it was determined that the

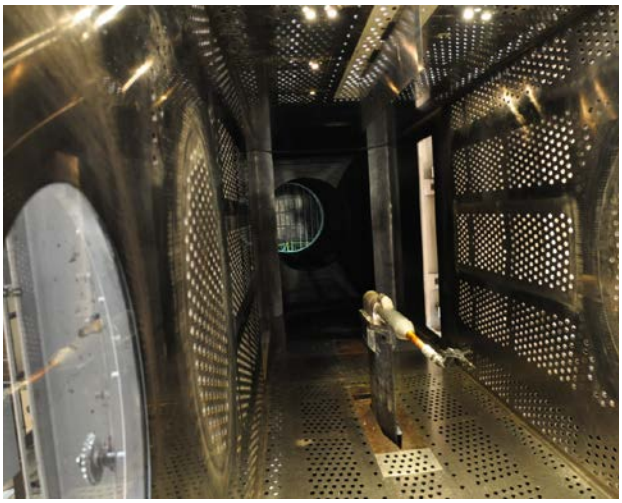

Figure 24 BM1 Model with the 14 inch Pressure Rail in the NASA Glenn 8'x6' Wind Tunnel

perforated window blank in the upstream section of the test was adding additional shocks, so the Schlieren window was swapped with it to provide cleaner flow in the test section. The Mach numbers tested ranged from 0.8 to 1.8 and the angles-of-attack ranged from -1 to +7 degrees. Figure 24 shows the BM1 sonic-boom model installed in the NASA Glenn 8’ x 6’ wind tunnel. The layout for the test is shown in Figure 25.

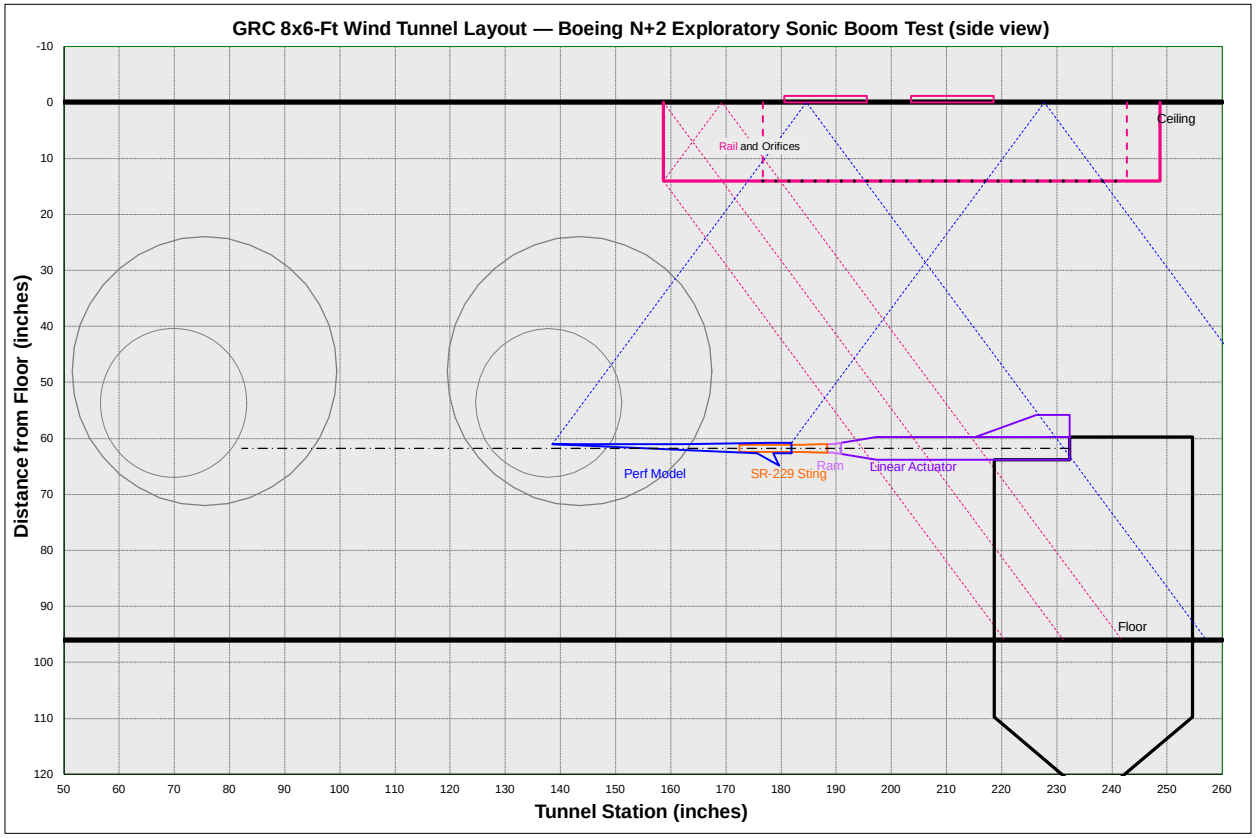

Figure 25 NASA Glenn 8' x 6’ Wind-Tunnel Layout for the Exploratory Test

V. Validation Analysis and Results

Validation analysis consisted of correlating pre-test CFD results with test data conducted in Phase I and II. In Phase I. the validation utilized three wind tunnel tests, the rail validation test, low-boom validation test, and parametric test. The plan was to validate the pressure measurement instrumentation with several calibration bodies and then utilize that instrumentation to conduct the low-boom concept validation. While validating the 14” Blade pressure rail, it became apparent that there was a significant variation in the results depending upon where the model was located in the wind tunnel. Several areas were investigated to determine the source of the uncertainty, including, height above the rail, longitudinal position in tunnel, whether the rail was on the forward or aft window blank, target humidity value, tolerance on holding humidity, and frequency of reference runs to minimize tunnel flow variations over time. Short term dP/P repeatability was within 0.007 for the lower heights (H < 32”) and 0.01 for the higher heights (H > 54”). Correlation with CFD was better in some locations then others, but captured the general shape and character of the data. The conclusion from the 14” rail validation test was that the instrumentation showed reasonable correlation, but the spatial and temporal variations were large enough that additional work was needed with the instrumentation and the test techniques.

It was believed that the 14” pressure rail may be partly responsible for the spatial and temporal variations due to the interference that the large rail provided to the measurements. This was later proven not to be true. However, to determine if the rail was responsible a smaller 2” tall flat-top rail was designed and built for the Phase I low-boom concept validation testing. A secondary reason for the change to a 2” rail was to maximize the H/L that could be tested for both the small sonic-boom model and the larger performance model. During the Phase I low-boom validation test, the 2” pressure rail was validated in a similar manner as the 14” rail using three different calibration

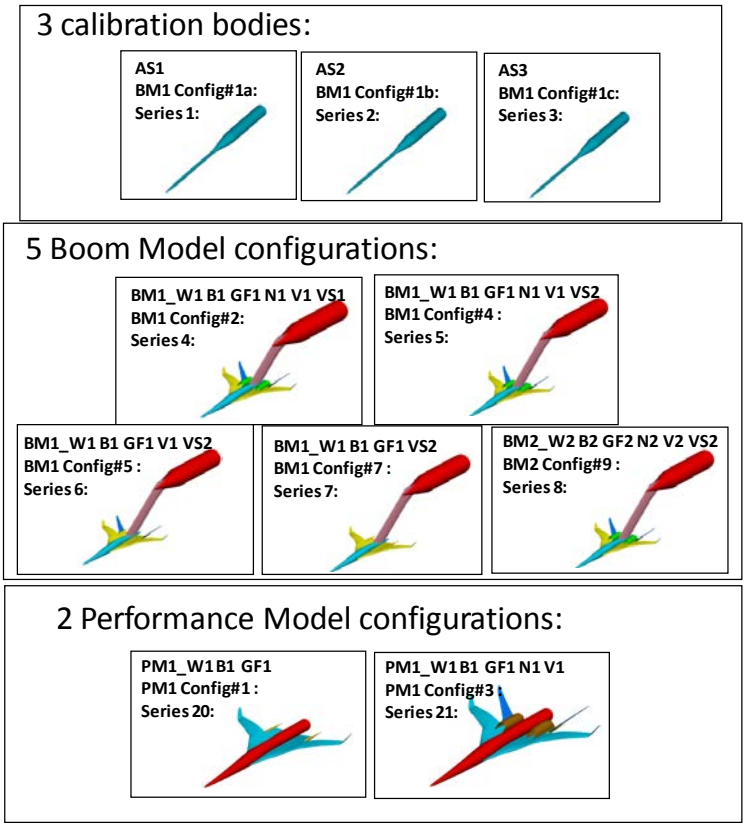

Figure 26 Ten Test Configurations were Utilized in the Phase I Validation

bodies with known near-field pressure distributions. Low-boom concept validation commenced after the 2"rail was calibrated.

From the Phase I low-boom validation test, a subset of the configurations tested in the wind tunnel were utilized for the validation analyses. The specific cases utilized for the validation are contained in Figure 26.

Comparisons with Euler CFD for the body-of-revolution models are contained in Figure 27. The CFD solutions had a few corrections made to them to account for the rail reflection factor and the fact that the pre-test CFD was conducted at a slightly different height than the data was measured. The reflection factor used was 1.3 to account for the signal reflection off of the 2" pressure measurement rail's flat top (note: the 14" pressure rail has a reflection factor of 1, because of its sharp edged top). The CFD signal was also scaled by a factor of 30 inches / 24 inches to account for the difference in height between the available CFD results and the wind-tunnel data. The figure includes comparisons for both Mach 1.6 and 1.8. The AS3 comparison is very good. The AS1 and AS2 comparisons are good, but there are some differences that may be attributed to rail interference and signal reflections off the wind-tunnel walls. The figure shows a representative comparison between the CFD and the test data for the rail calibration bodies. However, there was significant spatial variation of the results similar to what was observed for the 14" rail validation test.

Sonic-boom model comparisons between CFD and wind-tunnel data are shown in Figure 28. In this figure, comparisons are shown for the BM1 and BM2 wind-tunnel models at Mach numbers of 1.6 and 1.8. The distance between the models and the rail is 24 inches. These comparisons also include the rail reflection factor of 1.3 and the adjustment (30 inches / 24 inches) to account for the difference in height between where the CFD was conducted and where the measurements were taken. The angle-of-attack is approximately 3.6 degrees in all of the plots. The agreement with the test data is generally good. However, not all of the small features are captured in the comparison and the influence of the support hardware for the BM2 model at Mach = 1.6 does not show the best agreement. As with the BOR models, there were some variations in the comparisons depending upon the spatial location of the model in the wind tunnel.

The performance model sonic-boom comparisons between CFD and the wind-tunnel data are shown in Figure 29. Comparisons are shown for the wing/body configuration and the complete configuration at Mach numbers of 1.6 and 1.8. The model is located 60 inches above the pressure rail with an angle-of-attack of ~3 degrees for all of the figures. CFD analysis was conducted for two specific model support scenarios, a straight sting from the end of the model and a stepped sting which is more representative of the model installation. Agreement between the wind-tunnel data and the CFD is reasonable, although the CFD does not seem to capture a significant number of small shocks that are present in the data, especially in the front portion of the near-field signatures. The CFD result for the straight sting also does a poor job of capturing the aft signature near the support hardware. However, the CFD result for the stepped sting does a much better job in that area of the comparison. As with the BOR models and the sonic-boom models, the performance model correlations show the same spatial variation in the measured near-field pressures.

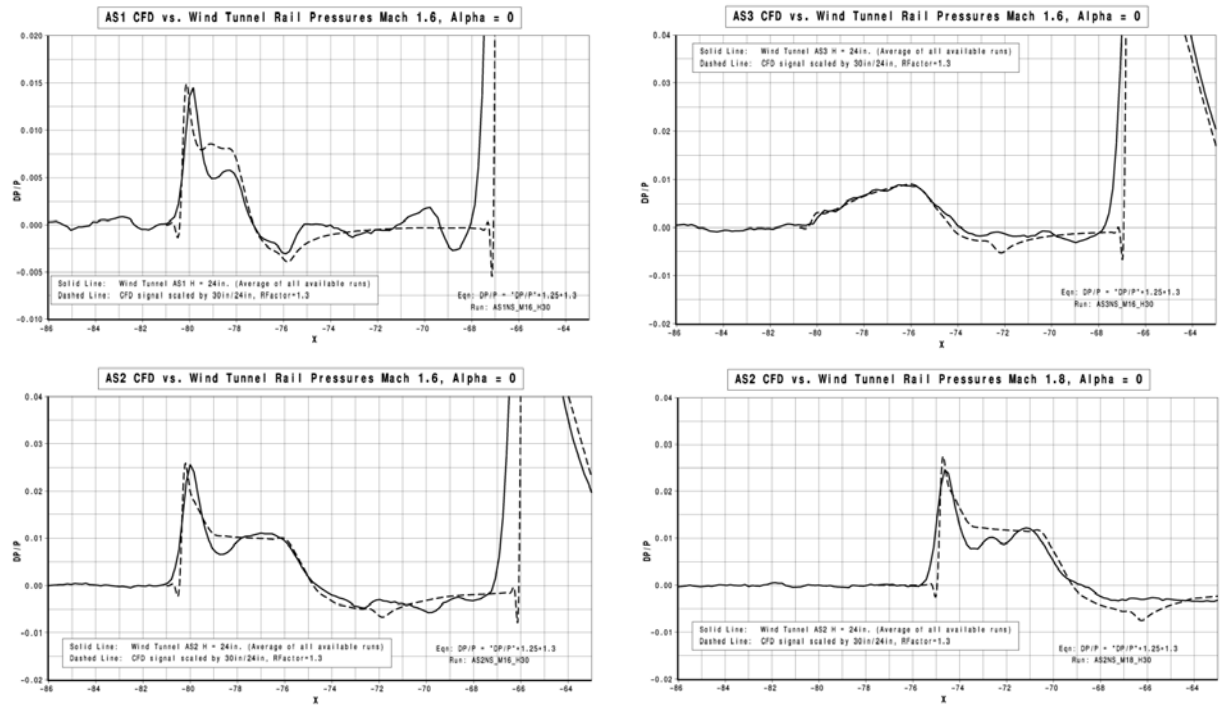

Figure 27 CFD Comparisons with NASA Ames 9' x 7' Wind-Tunnel Data and Boeing Body-of-Revolution CFD

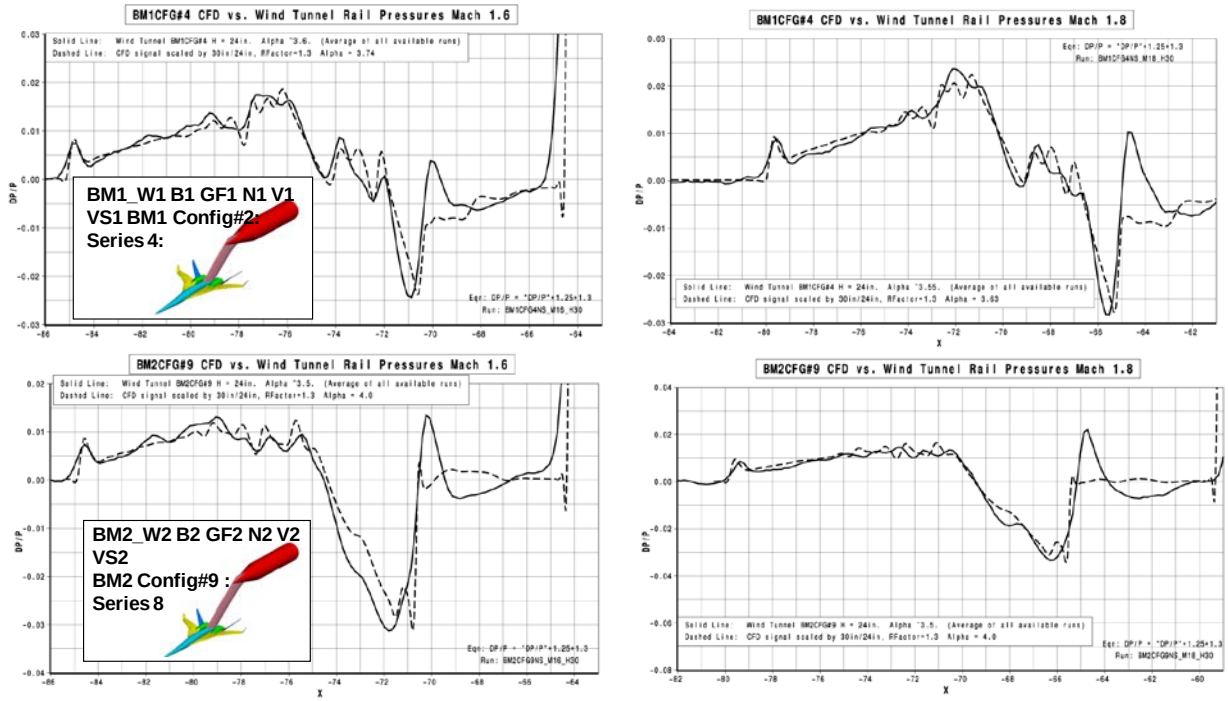

Figure 28 Sonic-Boom Model Comparisons between CFD and NASA Ames 9' x 7' Wind-Tunnel Data

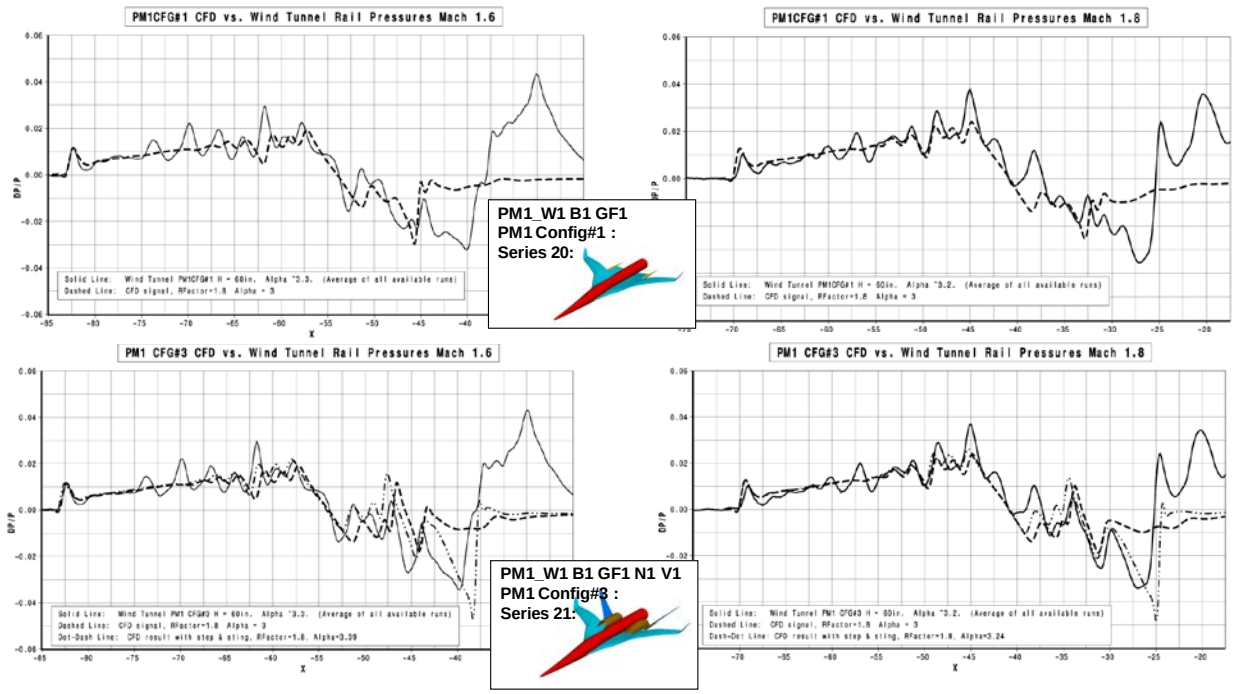

Figure 29 Performance Model Sonic-Boom Comparisons between CFD and NASA Ames 9' x 7' Wind-Tunnel Data

The Phase I validation test was one of the first low-boom configuration validation wind-tunnel tests in the N+2 Experimental Validation program. Sonic-boom wind-tunnel test results prior to this were measured for configurations that had much larger near-field pressure distributions. Variations in the signature with spatial location were not recognized as an issue, because they were small in comparison to the magnitude of the overall signature. However, the magnitude of the low-boom concept near-field signature is much smaller resulting in the spatial variation being a much larger percentage. Analysis of the Phase I Validation Test data and the 14" Rail Validation Test data were instrumental in determining the source of the spatial variation and helped determine a method to remove it from the data.

Boom signal data on the rail has shown a significant number of interferences even though a reference run has been used to tare the rail pressures to the test section static conditions. These interferences can be caused by the shielding effect of the model when it is above the rail, or reflections from the model, or other unknown sources. It is also believed that the spatial variation effect on the measured near-field pressures are a result of flow distortions from the spatial variation of Mach number in the test section [12]. A method for removing the spatial variations from the near-field pressure measurements (Spatial Averaging) was developed by researchers after the Phase I Low-Boom Validation test. The method is described in Reference 12. It mitigates the interference by gathering signal data at several model locations and then averaging to get a final signal. Typically several positions are taken in the fore-aft direction for an 'X-sweep', or in the vertical direction for a 'Z-sweep'. Equally good results are obtained whether you do an X-sweep or Z-sweep.

Spatial averaging was investigated in the Parametric Test. In this test, the BM1 and AS2 models were tested using the 14" blade rail. Both X-sweeps and Z-sweeps were conducted during the test. The results indicate good correlation with CFD. Figure 30 shows the correlation between the data and CFD at Mach 1.6 and a nominal height of 30 inches. Both Navier-Stokes and Euler results are shown in the comparison with the Euler results showing the best agreement with the data. The Navier-Stokes CFD results were fully turbulent and the boundary layer for the AS2 model was not artificially tripped. A significant portion of the model probably had a laminar boundary layer. The results match both shape and magnitude for the Euler comparison. A bow shock reflection off of the wall can be seen in both X-sweep (X= ~83 inches) and Z-sweep (X= ~88 inches) plots. However, this appears to be the only major rail interference in the measured data. Based on these comparisons, the 14"pressure rail is validated as a more accurate measurement device for sonic-boom testing.

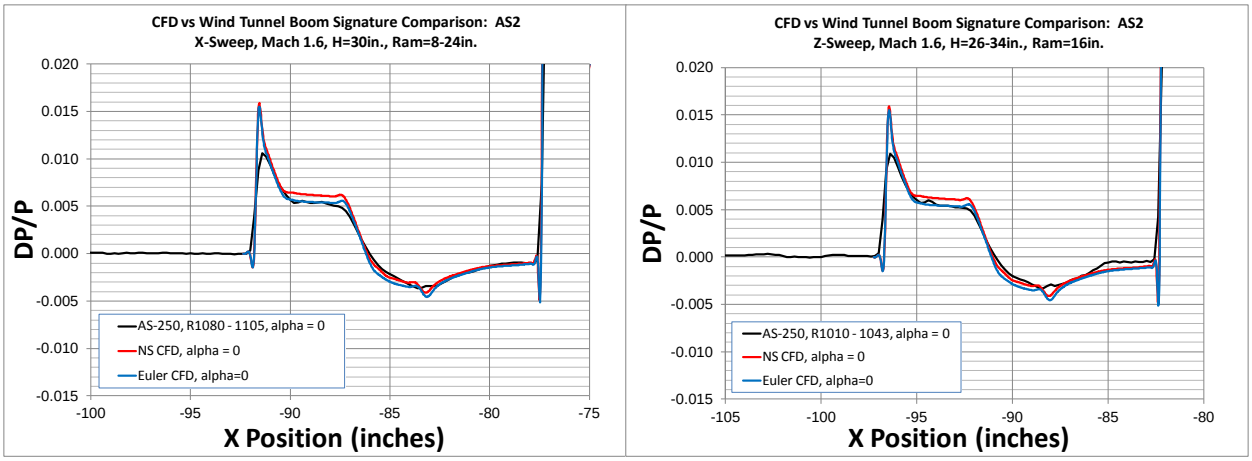

Figure 30 AS2 X-sweep and Z-sweep Spatial Averaged Results from the Parametric Test Validate the 14" Pressure Rail

Improved CFD correlations for the BM1 model were also observed during the Parametric Test. Figure 31 shows a comparison between the Parametric Test X-sweep and Z-sweep spatially-averaged results and Navier-Stokes CFD at Mach 1.6 and a nominal height of 30 inches. The Z-sweep correlation is better than the X-sweep in several areas, but both X-sweep and Z-sweep results tend to damp out the oscillations that the CFD shows in the areas near X=-83 to -88 inches for X-sweeps and X=-87 to -93 inches for Z-sweeps. It is uncertain why the signal is damped out in these areas, but potentials reasons include, wind-tunnel model fidelity, aeroelastic effects, improper CFD grid resolution, CFD numerical scheme, and number of locations in the spatial average. Also, the signal damping is more severe the farther you are from the pressure measurement rail. The results at 60 inches from the rail were rounded over to a greater extent and did not agree as well with CFD as the closer in-rail measurements.

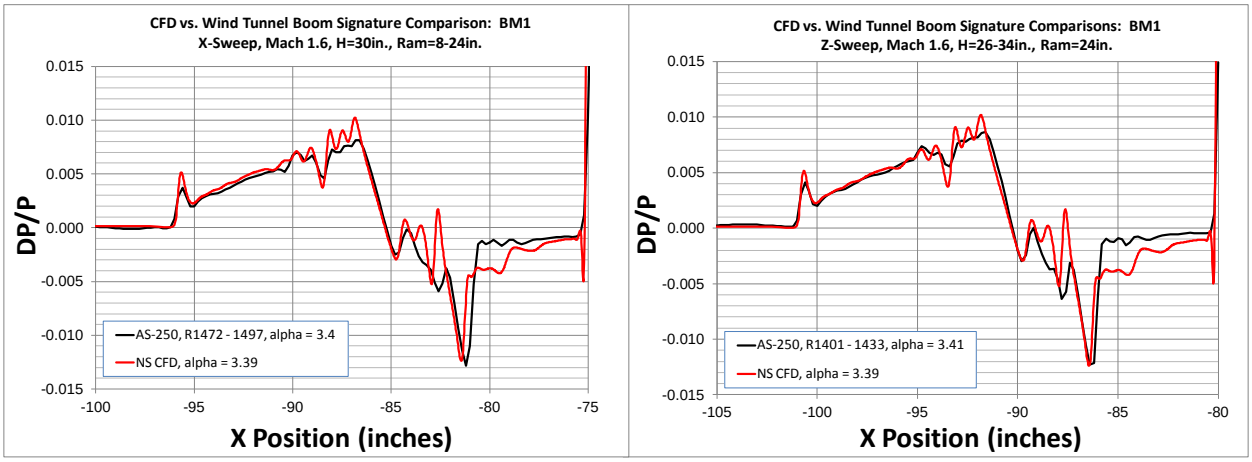

Figure 31 BM1 X-sweep and Z-sweep Spatial Averaged Results from the Parametric Test Show Improved Correlation Over Results from the Low-Boom Validation Test

To determine if aeroelastics were responsible for some of the disagreement, additional CFD was run with the wing linearly deflected from 0 degrees at the start of the wing outboard panel to -2 degrees at the wing tip. From past work on the HSR program, it was determined that 95% of the aeroelastic effect occurred on the wing outboard panel. In the wind tunnel, the wing outboard panel is both translating in Z and twisting. Here, we are just considering the twist component. The -1 degree deflected case was also run. Figure 32 contains the BM1 CFD correlation at Mach 1.8 and a nominal height of 30 inches. Both the X-sweep and Z-sweep spatially averaged data show improved correlation for the estimated -1 and -2 degree aeroelastic effect on the wing. The -1 degree estimated aeroelastic effect shows the best correlation with the data in the -80 to -85 inch X position location for X-sweeps and -85 to -90 inch X position location for the Z-sweeps.

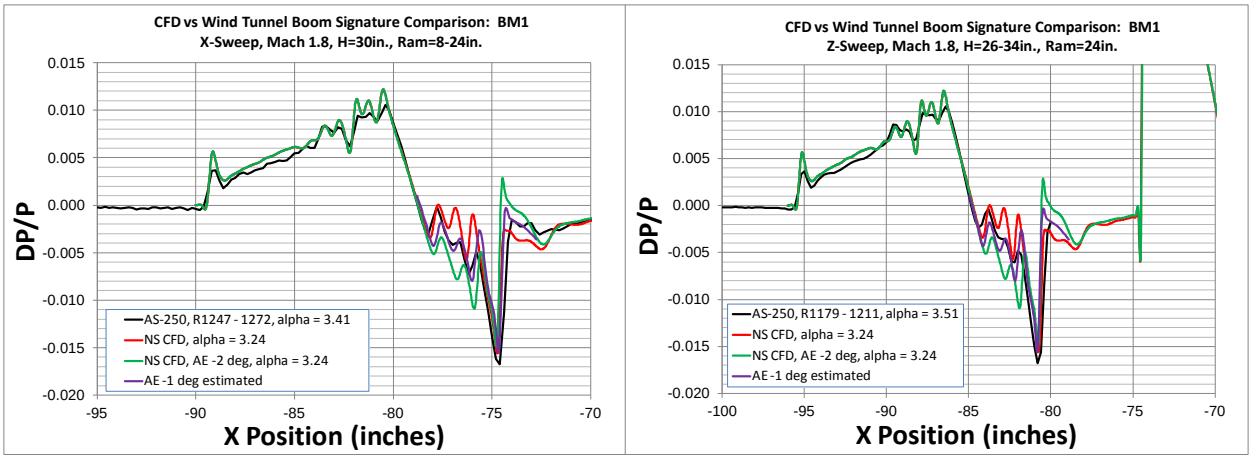

Figure 32 Simulated Aeroelastic Affects Show Improved Correlation in the Aft Portion of the Sonic-Boom Signature at Mach 1.8 and a Nominal Height of 30 inches

Figure 33 shows all of the signatures in an X-sweep series from the Parametric Test at Mach 1.6 and a nominal height of 30 inches. The averaged result is also contained in the black line on the plot. It is possible that by acquiring data for longitudinal movements that cover 4 pressure taps may damp out some of the signal. Additional step sizes (every 2 or 3 pressure taps) may provide fidelity in the areas of the plot that do not correlate well with CFD. More testing and CFD analysis is required, but from the Parametric Test data set, the low-boom concept validation is reasonable.

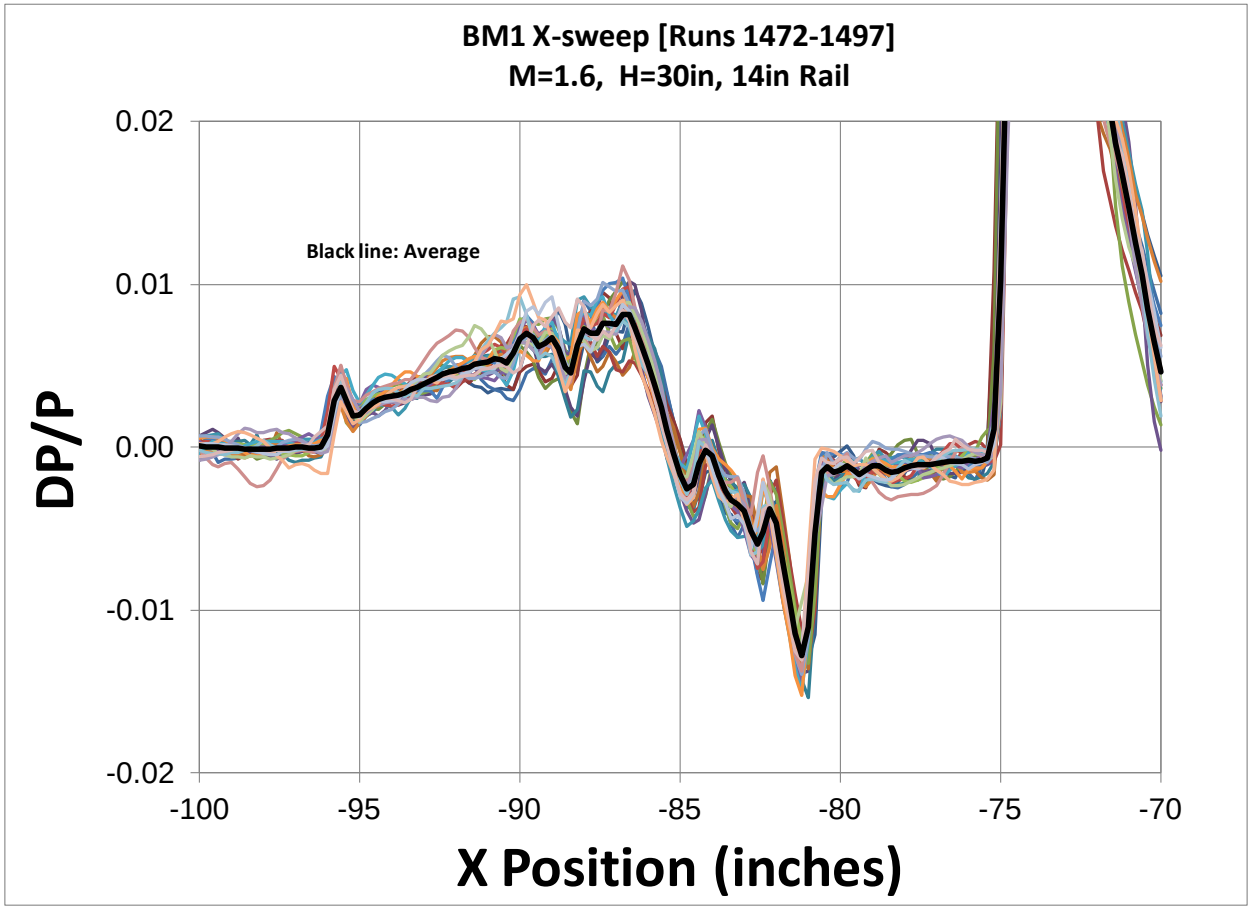

Figure 33 BM1 Composite X-sweep Results Show the Total Spatial Variation in the Near-Field Pressure Distribution at Mach 1.6 and Nominal Heights of 30 inches

At the end of the Parametric Test, the correlation with CFD and wind-tunnel data for the low-boom concept was fairly good. Many of the issues that came up in the Rail Validation and Low-Boom Validation tests were solved with the spatial-averaging test technique. However there still were some areas in the BM1 near-field pressure distribution that did not correlate very well. Also, the effect of propulsion integration on the near-field signature validation needed to be investigated. The propulsion integration effects required a larger Mach range to validate both the sonic-boom and the inlet performance, so alternate facilities were investigated in two short exploratory tests, one at NASA Ames 11' wind tunnel and the other at the NASA Glenn 8' x 6' wind tunnel. The goal of each test was to determine how to get good near field and aerodynamic performance results in each facility.

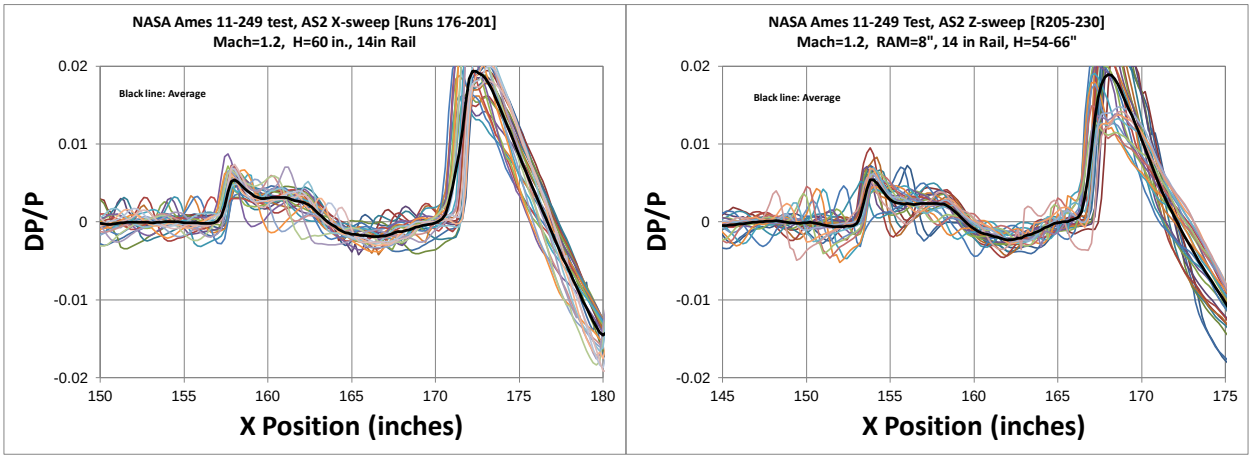

Figure 34 NASA Ames 11-249 Test Data Shows That Spatial Averaging Provides Similar Results for the AS2 Model at Mach 1.2

Running at the Ames 11' presented some problems that were unforeseen during test preparation. The support system exhibited dynamics at Mach numbers above 1.2, and testing was limited by the internal balance limits being exceeded by the inertial loads of the model during the dynamics. Some limited data was recorded at the lower Mach numbers; however the boom signatures may be suspect due to excessive model movement. A sample of this data is included in Figure 34 for the AS2 model. The spatial averaging appeared to work as it did in the parametric test. However, no CFD was conducted at this lower Mach number for comparison. Further investigation into the support hardware dynamics was deemed beyond the scope of the exploratory test goals. While the data quality from the Ames 11' test was not ideal, the productivity of the facility was similar to the Ames 9'x7'.

The majority of the test time during the Glenn entry was spent fine-tuning the process for producing good sonic-boom data. The lessons learned included the importance to holding a tight Mach tolerance during the sonic boom measurements, and also accounting for the effect of the weather on the available supply of dry air. In general, once these processes had been implemented, the results seemed reasonably good. The data quality of the NASA Glenn 8'x6' Test was at least as good as the NASA Ames 9'x7' Parametric Test, however the facility productivity was limited by the capacity of the desiccant beds to provide dry air.

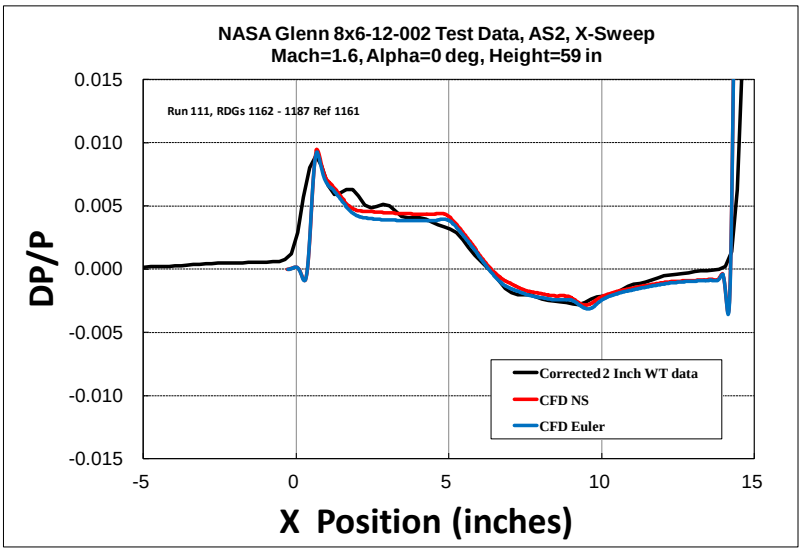

Figure 35 Glenn 8'x6' Results for AS2 Body-of-Revolution Model

Figure 35 shows results for the

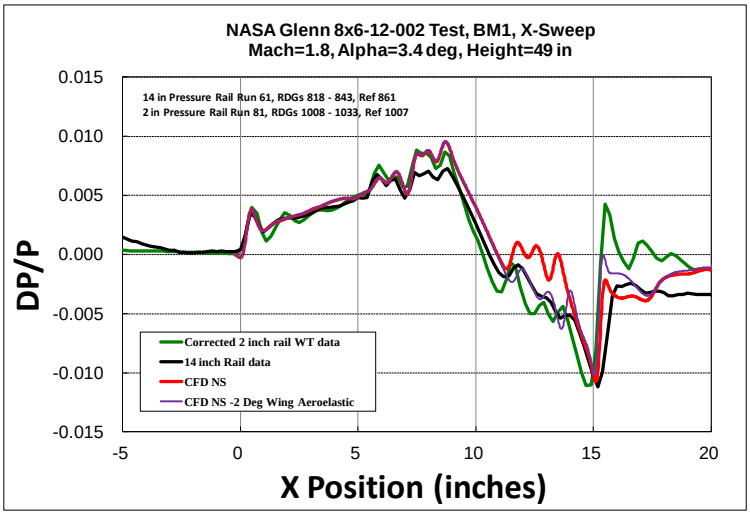

Figure 36 NASA Glenn 8' x 6' Near-Field Pressures Show Similar Results to those acquired at the NASA Ames 9' x 7' for the BM1 Model with Simulated Aeroelastic Effects

AS2 body-of-revolution, at Mach 1.6 and a height above the 2 inch pressure rail of 59 inches, compared with CFD. The CFD comparison cases are Navier-Stokes and Euler solutions. For these cases the wind tunnel data shows some oscillations where CFD is showing a flat-top near-field signature. These oscillations are the bow shock wave reflected off of the wall at X=2" to 3". The CFD solutions also show a steeper nose shock onset, although some of this may be due to model movement.

Figure 36 shows the results for the BM1 model at Mach 1.8 at a height above the rail of 49 inches (h/l ~3.5). The 14 inch rail data shows fairly good agreement on the front part of the signal while the 2 inch corrected signal picks up the peak levels better. Both pressure rails tend to miss the aft part of the signature compared to CFD, so an additional CFD signal is plotted which has a -2 degree outboard wing washout to estimate the amount of wing and model deflection under load in the wind tunnel.

The results of the exploratory tests showed that the NASA Glenn 8'x6' is a viable facility for sonic boom and force testing over the Mach range of interest. The NASA Ames 11' was not able to cover the full Mach range due to support system dynamics; however some further work at that facility could be done to rectify those issues. The NASA Glenn facility was not without its issues with productivity, but the data quality was good.

Performance model lift, drag, and pitching moment comparisons between CFD and wind-tunnel data are shown in Figure 37. The test and CFD were run at Mach 1.8 for the complete performance model configuration. Cruise drag compares within 1 – 2 drag counts. Lift and pitching comparisons are very good. The aerodynamic performance test techniques were worked extensively during the High Speed Research (HSR) program. As with HSR, the aerodynamic performance correlations were very good.

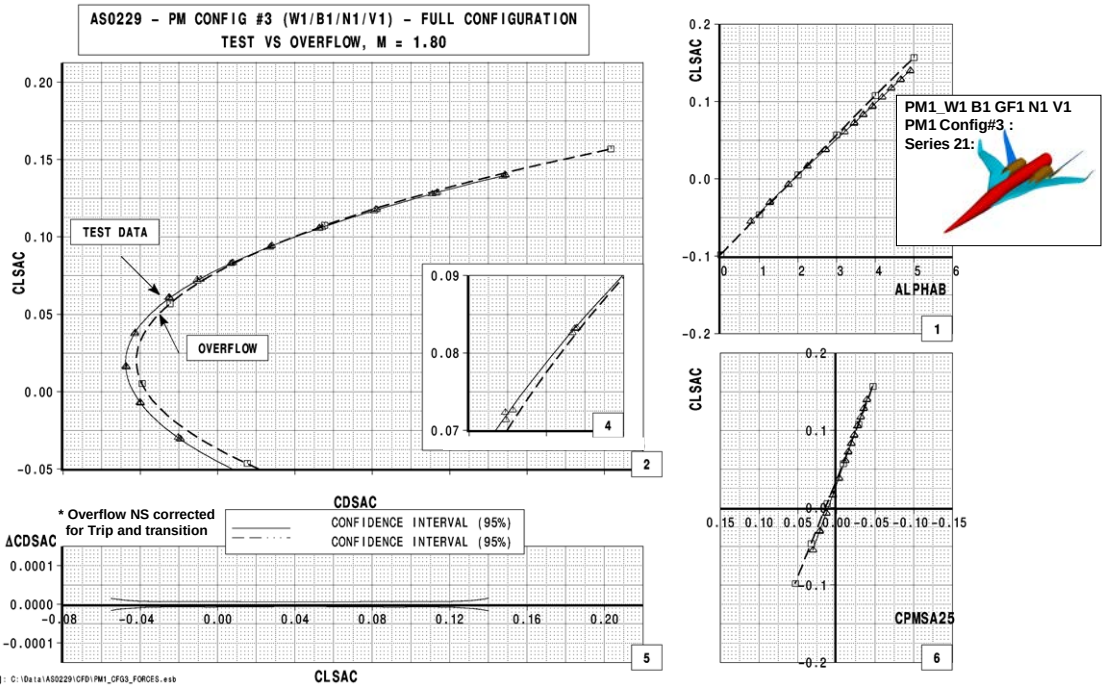

Figure 37 Performance Model Lift, Drag, and Pitching Moment Comparisons between CFD and NASA Ames 9' x 7' Wind-Tunnel Data

VI. Conclusions and Future Work

The Boeing N+2 Experimental Validation project has been very successful. The project has demonstrated the predictive capability to assess signatures and aerodynamic performance of an N+2 generation supersonic commercial aircraft. We have demonstrated low-boom design capability to achieve an overland sonic-boom of 81 PLdB with progress toward the longer-term goal of 65-70 PLdB. An extensive set of validation data has been gathered from which CFD tools have been validated. We have also delivered an extensive set of modular models to NASA for continued research to calibrate instrumentation and facilities. The project has provided and developed two new pressure measurement rails, which have been validated in several wind-tunnel tests. The 14" blade rail was selected as the rail of choice, because the rail reflection factor is 1 and the number of corrections required is small.

The low-boom concept validation has matured over five wind-tunnel tests. The spatial-averaging test technique provides good near-field pressure results at all of the facilities investigated. Both X-sweep and Z-sweep spatial-averaging provide equally good results. The low-boom concept has been validated, but there are areas in the near-field pressure distribution that do not match between data and CFD. The data in these areas appear to be damped out in comparison with the CFD. Larger damping is also observed in measurements taken at larger H/L position from the rail. Estimated aeroelastic effects resolve some of the areas of disagreement, but more work is needed to provide the best correlation. Additional improvements in test techniques may be required to better correlate with CFD.

Three wind-tunnel facilities have been evaluated so far in the validation effort, the NASA Ames 9' x 7' Supersonic Wind Tunnel, NASA Ames 11ft Transonic Wind Tunnel, and the NASA Glenn 8' x 6' Supersonic Wind Tunnel. All of the facilities provide good near-field pressure distributions using the spatial-averaging technique. However, with our particular model layout and support system, the model dynamics at the NASA Ames 11' wind tunnel was too severe to get the Mach 1.4 data we needed for the Phase II propulsion integration sonic-boom wind tunnel-testing.

The remaining work in the Boeing N+2 Experimental Validation project includes the Phase II propulsion integration testing and validation analysis.

Acknowledgments

The work described in this paper was conducted under NASA task order contract NNL08AA16B NNL10AA00T. The authors would like to thank Linda Bangert, David Richwine, Peter Coen, Don Durston, Maureen Delgado, NASA Ames 9' x 7' Wind-Tunnel Staff, Ray Castner, Stephanie Simerly, Stephanie Hirt, Scott Williamson and the NASA Glenn 8' x 6' Wind-Tunnel Staff for their professionalism and support through-out the N+2 Experimental Validation project. In addition we would like to thank Don Durston for his fantastic excel-based wind-tunnel test section layout files. The contributions of the following members from the Boeing team are also gratefully acknowledged: Eric Adamson, Chet Nelson, Alicia Bidwell, Kevin Mejia, Eric Unger, Dave Bruns, Stewart Lumb, Pete Wilcox, Larry Fink, Juan Cajigas, Dave Treiber, Tony Antani, and Bob Welge.

References

[1]Seebass, R., "Sonic Boom Theory," *AIAA Journal of Aircraft*, Vol. 6, No. 3, May-June 1969, pp. 177-184.

[2]Seebass, R., and George, A. R., "Sonic-Boom Minimization," *The Journal of the Acoustical Society of America*, Vol. 51, No. 2 (Part 3), 1972, pp. 686-694.

[3]George, A. R., and Seebass, R., "Sonic Boom Minimization Including Both Front and Rear Shocks," *AIAA Journal*, Vol. 9, No. 10, October 1971, pp. 2091-2093.

Darden, C. M., "Minimization of Sonic Boom Parameters in Real and Isothermal Atmospheres," NASA TN D-7842, March 1975.

[5]Darden, C. M., "Sonic-Boom Minimization with Nose-Bluntness Relaxation," NASA TP-1348, 1979.

[6]Aftosmis, M. J., Nemec, M., and Cliff, S. E., "Adjoint-Based Low-Boom Design with Cart3D," *29th AIAA Applied Aerodynamics Conference*, AIAA 2011-3500, Honolulu, Hawaii, June 2011.

[7]Park, M. A., "Low Boom Configuration Analysis with FUN3D Adjoint Simulation Framework," *29th AIAA Applied Aerodynamics Conference*, AIAA 2011-3337, Honolulu, Hawaii, June 2011.

[8]Rallabhandi, S., "Sonic Boom Mitigation Through Aircraft Design and Adjoint Methodology," *30th AIAA Applied Aerodynamics Conference*, AIAA 2012-3220, New Orleans, Louisiana, June 2012.

[9]Welge, R. H., Nelson, C., and Bonet, J., "Supersonic Vehicle Systems for the 2020 to 2035 Timeframe," *28th AIAA Applied Aerodynamics Conference*, AIAA 2010-4930, Chicago, Illinois, June 2010.

[10]Nichols, R. H., Tramel, R. W., and Buning, P. G., "Solver and Turbulence Model Upgrades to OVERFLOW 2 for Unsteady and High-Speed Applications," AIAA 2006-2824-824, 24th Applied Aerodynamics Conference, 5–8 June 2006, San Francisco, California.

[11]LeDoux, S. T., Herling, W. W., and Fatta, G. J., "MDOPT – A Multidisciplinary Design Optimization System Using Higher Order Analysis," *10th AIAA/ISSMO Multidisciplinary Analysis and Optimization Conference*, AIAA 2004-4567, 30 August – 1 September 2004.

[12]Morgenstern, J. M., "How to Accurately Measure Low Sonic Boom or Model Surface Pressures in Supersonic Wind Tunnels," *30th AIAA Applied Aerodynamics Conference*, AIAA 2012-3215, New Orleans, Louisiana, June 2012.

[13]Morgenstern, J. M., "Distortion Correction for Low Sonic Boom Measurement in Wind Tunnels," *30th AIAA Applied Aerodynamics Conference*, AIAA 2012-3216, New Orleans, Louisiana, June 2012.